Scholars' Mine

Masters Theses   Student Theses and Dissertations

1961

Analyses of two new electrode configurations for earth resistivity surveying

Chi-Chao Chang

Follow this and additional works at: https://scholarsmine.mst.edu/masters_theses

Part of the Mining Engineering Commons

Department:

Recommended Citation

ANALYSES OF TWO NEW ELECTRODE CONFIGURATIONS
FOR EARTH RESISTIVITY SURVEYING

BY

CHI-CHAO CHANG

————————

A

THESIS

submitted to the faculty of the

SCHOOL OF MINES AND METALLURGY OF THE UNIVERSITY OF MISSOURI

in partial fulfillment of the work required for the

Degree of

MASTER OF SCIENCE, MINING ENGINEERING

Rolla, Missouri

1961

————————

Approved by

James C. Maxwell (advisor) _Gerald B. Rupert_

ABSTRACT

Two new electrode configurations for the electrical resistivity surveying are introduced: the A-configuration, consisting of a closely spaced pair of current electrodes separated at larger distance from the closely spaced pair of potential electrodes, and the B-configuration, in which each closely spaced pair consists both current and potential electrode. Because electrode pairs can be carried as units, the new configurations can be applied to continuous resistivity surveying more easily than the Wenner configuration.

Equations derived for apparent resistivities are:

$$\rho_a = \frac{\Delta V}{I} \; 2\pi \left[\frac{r(r^2 - a^2)}{2a^2} \right] \qquad \text{for the A-configuration}$$

and

$$\rho_a = \frac{\Delta V}{I} \; 2\pi \left[\frac{ar}{2(r-a)} \right] \qquad \text{for the B-configuration}$$

Error in measurement of (r) affects accuracy of (ρ_a) more for A- than for B-configuration.

Theoretical apparent resistivity values are derived, by Maxwell's theory of images, for the A- and B-configuration over a two layered earth using the depth probe method, and across a vertical fault plane using lateral traversing. These theoretical values are substantiated by measurements of models.

ACKNOWLEDGEMENT

TABLE OF CONTENTS

LIST OF FIGURES

LIST OF TABLES

I. INTRODUCTION

The electrical resistivity method of geophysical prospecting essentially involves passing a current I (See Fig. 1-1) through the earth by means of two current electrodes, C_1 and C_2, measuring the resulting potential difference $\triangle V$ between two potential electrodes, P_1 and P_2, and calculating the conducting properties of the subsurface from the measured resistance $R = \triangle V/I$. The lithology and structure of the underlying earth material is interpreted from the apparent resistivity which is calculated from the measured resistance cf the earth.

Mathematical analysis can be used to solve for values of apparent resistivity for assumed ideal cases. Such analysis aids the interpretation of actual field data. Mathematical study is used to analyze various electrode arrangements for the development of new techniques (CARPENTER, 1955, for example). This thesis is a mathematical study of two new electrode configurations.

Widely employed electrode configurations have been illustrated and explained in many previous papers (HUBBERT, 1934; HEILAND, 1940; JASKOSKY, 1957). The most commonly adopted electrode configuration has been that due to WENNER (1915). The four electrodes are placed at equal intervals along a straight line on the surface of the earth, as shown in Fig. 1-1.
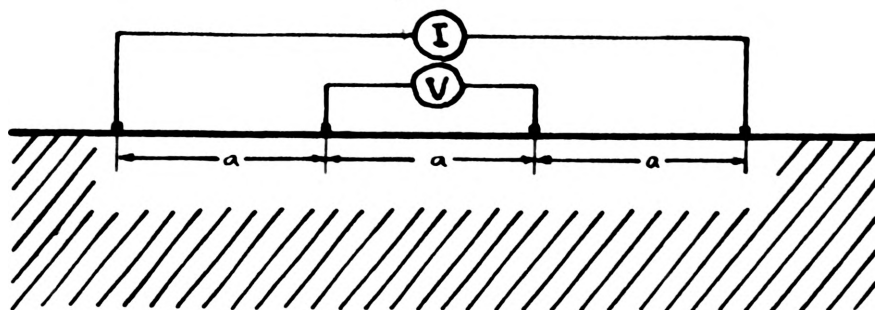
Fig. 1-1 Electrode configuration
   for electrical resistivity
   method.

Two techniques for applying the Wenner electrode configuration
can be distinguished, namely traversing and probing . In the former
method the electrode spacing (a) is held constant and the system as
a whole is moved over the surface of the earth. The movement is
usually made either along the line of the electrodes (longitudinal
traversing) or perpendicular to it (transverse traversing). In the
depth probing method the line of the electrodes is fixed in direction
and the spacing (a) is varied, keeping the centre of the electrode
line at the same point. These two techniques can be applied to
other configurations.

Mathematical analysis of resistivity measurements is based on
some simple assumptions and relationships which are true for all
electrode configurations. The current electrodes may be treated as
point sources of equal and opposite strength. For the purpose of
this thesis C_1 will be considered to be the electrode at which the
current of strength (+I) enters the earth. $\triangle V$ is defined as the

potential difference between P_1 and P_2. Therefore

$$\Delta V = (\text{Potential at } P_1) - (\text{Potential at } P_2)$$

$$= V_1 - V_2 \qquad\qquad 1\text{-}1$$

It will be necessary, in general, to specify its sign as well as its magnitude. The distance between any two electrodes can be expressed by the symbols of the electrodes at the end points, such as C_1P_1, C_2P_2, C_1P_2, etc.

For the interpretation of experimental results the value of apparent resistivity (ρa) can be obtained by substituting the relevant values in the equation

$$\rho a = 2\pi RF \qquad\qquad 1\text{-}2$$

where

$$R = \frac{\Delta V}{I} \qquad\qquad 1\text{-}3$$

$$F = \left[\frac{1}{C_1P_1} - \frac{1}{C_1P_2} - \frac{1}{C_2P_1} + \frac{1}{C_2P_2} \right]^{-1} \qquad\qquad 1\text{-}4$$

R is the value measured directly from instruments and is called the configuration resistance. F is the multiplying factor for the electrode arrangement and is called the configuration factor. Regardless of the electrode configuration employed, the potential at an electrode (P_n) is, from equation 1-2,

$$V_n = \frac{I\rho a}{2\pi} \left[\frac{1}{C_1P_n} - \frac{1}{C_2P_n} \right] \qquad\qquad 1\text{-}5$$

This thesis introduces two new electrode configurations. In both configurations four electrodes are used, grouped in pairs. For one arrangement a current and potential electrode are placed close together at a relatively large distance from another current-potential pair. The other arrangement consists of two current electrodes placed close together at a relatively large distance from two closely spaced potential electrodes.

Equations for computing potential differences and apparent resistivity are derived for each configuration. Theoretical considerations and calculations are made for two assumed simple geologic conditions and mathematical solutions are given. Comparisons of sensitivity of the new configurations to lateral and vertical changes in earth resistivity and to changes in electrode spacing are made with that of the Werner configuration. Both new configurations were used in experimental measurements of resistivity of three-dimensional models which simulated simplified geologic conditions.

II. RESUME OF THEORY

The basic procedure of the electrical resistivity method is to pass a measured electric current through a selected portion of the earth and measure the potential drop or some other electrical quantity associated with this flow of current. This is usually accomplished by passing the current between energizing electrodes placed at selected points in the area under investigation. For convenience in the interpretative analysis, usually all the electrodes are placed in a straight line. From the observed values of the current and potential, the apparent resistivity of the material included within the zone of measurement can be calculated for any given electrode configuration. Furthermore, calculations can be made for certain assumed simple geologic conditions by solving Bessel functions (MAEDA, 1955) or applying Maxwell s theory of images (JEANS, 1925). These theoretical values are the basis of interpretation of the obtained field data.

A. Fundamental Equations.

Consider the case where electric current is introduced into an infinitely homogeneous and conductive medium by a point current source placed inside the medium. The medium is conductive, therefore the introduced current will distribute into the medium equally in all directions. If the introduced current is (I) and the resistivity of the medium is (ρ), the total current flowing out of the current source is (I). Because the distribution is equal in all directions, the distribution is spherical with the current source as its center. The original current strength introduced into the medium is I, therefore

the current strength at any point distance (r) from the current source is $1/4\pi r^2$. This is called the "current density" and designated as (i), i.e.,

$$i = \frac{I}{4\pi r^2} \qquad 2\text{-}1$$

According to Ohm's Law, the distribution of electric current in a resistive medium will produce potential drop. The potential gradient (dV/dr) is stated as the rate of change of potential with small increment of distance. Ohm's Law states that

$$\frac{dV}{dr} = -\rho i \qquad 2\text{-}2$$

where (ρ) is the resistivity of the medium. Combining above equations,

$$\frac{dV}{dr} = -\rho \frac{I}{4\pi r^2} \qquad 2\text{-}3$$

By integrating, we obtain the total potential value around that particular point,

$$V = \rho \frac{I}{4\pi r} + C \qquad 2\text{-}4$$

At infinity the potential must be zero, so the constant C is zero and

$$V = \rho \frac{I}{4\pi r} \qquad 2\text{-}5$$

B. Theory of Images.

If the medium is not homogeneous, the current distribution is not uniform in all directions. The boundary of two different media will produce many effects in current distribution. The mathematical solution for this two-media case can be solved by the application of Maxwell's theory of images (JEANS, 1925; JAKOSKY, 1957).

If a difference in resistivity exists on a formation boundary (see Fig. 2-1) its effect may be represented by placing a plate with definite transmission and reflection characteristics at the boundary. Assume a current source distant at (P) above the plate. Considering the phenomenon for the moment as one of light transmission, an observer at (A) facing the plate would see the point (P) by looking at its image (I). The light at (A) would be that received directly from (P) plus the amount reflected by the plate and appearing to come from the image (I). If the dimming of the apparent source at (I), due to reflection, be indicated by a factor (k), the light and by analogy the potential at (A) is equal to the amount at the source diminished by the geometric effect of distance (I/r) plus the amount reflected, so

$$V_A = \frac{\rho_1 I}{4\pi}\left[\frac{1}{r_1} + \frac{k}{r_2}\right] \qquad 2\text{-}6$$
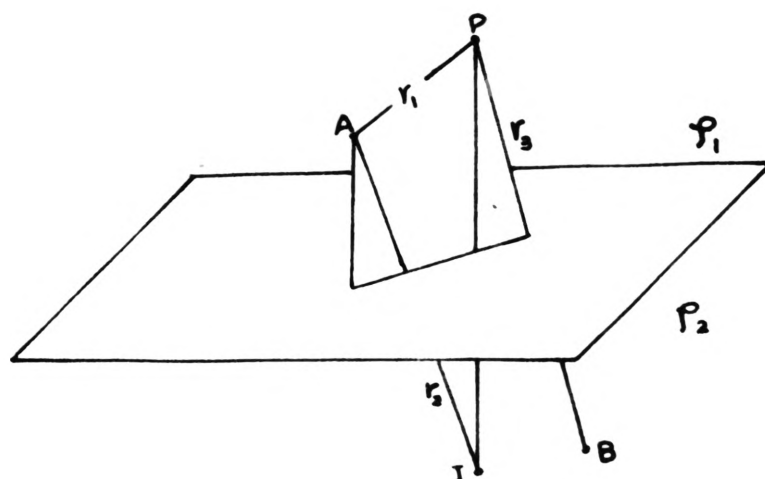
Fig. 2-1 Conditions on Boundary Between
Two Media of Different Resistivity

An observer facing the plate at (B) sees the source (P) at an intensity reduced by transmission through the plate. The amount transmitted is the original intensity minus the amount lost through reflection, which inturn is proportional to (k) times the original intensity. Therefore, the light and by analogy the potential at (B) is

$$V_B = \frac{\rho_2 I}{4\pi r}(1-k) \qquad 2-7$$

Continuity of the potential requires that in the boundary plane where $r_1 = r_2 = r_3$, V_A and V_B are equal, at the boundary $\frac{1}{\rho_1}\frac{V_1}{n} = \frac{1}{\rho_2}\frac{V_2}{n}$

where n is taken along the direction normal to the boundary. Therefore

$$\frac{\rho_1 I}{4\pi r}(1+k) = \frac{\rho_2 I}{4\pi r}(1-k)$$

hence

$$\qquad\qquad 2-8$$

$$k = \frac{\rho_2 - \rho_1}{\rho_2 + \rho_1}$$

$$1-k = \frac{2\rho_1}{\rho_2 + \rho_1}$$

$$1+k = \frac{2\rho_2}{\rho_2 + \rho_1}$$

The factor (k) expresses the hypothetical "electrification" of a plane between two media of different resistivities due to a point source and its image. This factor is called the "reflection factor". Usually the reflection factor between earth and air is a special factor, because the resistivity of air is infinite, and is designated as (k'). Thus

$$k' = \frac{\rho_{air} - \rho_1}{\rho_{air} + \rho_1} = \frac{1 - \rho_1/\rho_{air}}{1 + \rho_1/\rho_{air}}$$

or

$$k' = \frac{1 - \frac{\rho_1}{\infty}}{1 + \frac{\rho_1}{\infty}} = 1 \qquad 2-9$$

C. Single Layer Problem.

Application of this principle of continuity at a boundary is illustrated by a calculation of the potential distribution resulting from two current electrodes beneath the ground surface. This theoretical problem corresponds to a field application of a four-electrode configuration with buried electrodes (Fig. 2-2). If the point (A) is considered as current source (I) and (B) as the corresponding current sink (-I), the potential distribution at the surface is obtained by considering the effects of both sources, (A) and (B), and their images, (A′) and (B′). The intensities of the images are (k′I) and (-k′I), respectively. Applying Equation 2-9, (k′) is seen to be equal to 1. Hence, the images have the strength (I) and (-I), respectively.   The potential difference between (P) and (Q) due to a source of strength (I) at (A) is

$$\Delta V = \frac{\rho_1 I}{4\pi} \left[\frac{1}{AP} - \frac{1}{AQ} \right] \qquad \text{2-10}$$

and that due to an image I at A′ is

$$\Delta V = \frac{\rho_1 I}{4\pi} \left[\frac{1}{A'P} - \frac{1}{A'Q} \right] \qquad \text{2-11}$$

Similar relations apply to the potential difference at the same points resulting from the source at (B) and its image at (B′). These potential difference are

$$\Delta V = \frac{\rho_1 I}{4\pi} \left[\frac{1}{BP} - \frac{1}{BQ} \right] \qquad \text{2-12}$$

$$\Delta V = \frac{\rho_1 I}{4\pi} \left[\frac{1}{B'P} - \frac{1}{B'Q} \right] \qquad \text{2-13}$$
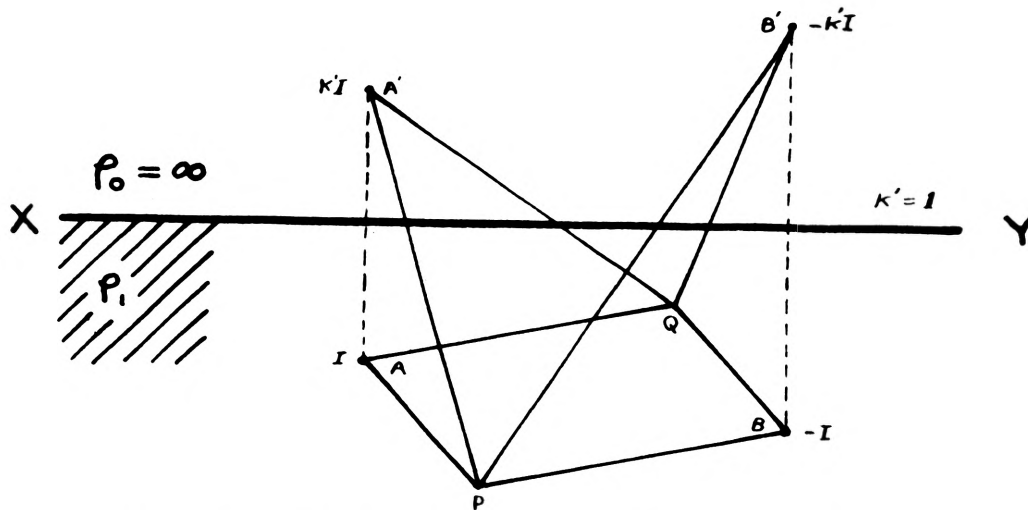
Fig. 2-2 Four Points and Images on Boundary

As electrodes approach the ground surface, or the boundary, the electrodes and their images approach each other and finally combine to become points having both current strength and reflected strength at the boundary. $I' = (1+k)I$. If the upper medium is air, for the field method, the resistivity of the air is infinite so the reflection factor is $k' = 1$. Thus equation 2-10 becomes

$$\Delta V = \frac{\rho I}{2\pi}\left[\frac{1}{AP} - \frac{1}{AQ}\right]$$

2-14

with similar changes in the other three equations. For the electrical resistivity calculations it is more convenient to think of the current distribution from a source on the surface of the earth as being in a 2π or hemispherical direction.

D. Two Layer Problem.

The two layer problem is an extention of the single layer problem. The two layer problem consists of two boundaries separating three media. For the geophysical case the upper boundary is the boundary of the air and earth, having a reflection factor of (k'). Mathematical solutions can be obtained by applying Maxwell's theory of images (ROMAN, 1930, 1933, 1953, 1959, 1960) or applying solutions by Bessel functions (MAEDA, 1955). However, image solution is easier to understand, hence many solutions have been achieved by this method.

Consider a uniform layer (1) of thickness (d) and resistivity (ρ_1) overlying a semi-infinite homogeneous medium (2) of resistivity (ρ_2) (Fig. 2-3). This geological two-layer structure corresponds to an electrical three-layer problem, the upper layer of which has a resistivity of $\rho_o = \infty$. Assume that a current source I_0 and a sink $-I_0$ are located at the boundary of media 0 and 1.

Solution of the current and potential distribution is facilitated by considering the effects of the source and sink independently and then combining them. Furthermore the solution for the potential due to the sink ($-I_0$) at any point on the line passing through the source and sink can be obtained from the solution for the potential due to the source (I_0) by replacing (x), the distance of the point from (I_0), by (L-x) where (L) is the distance between the source and sink. Thus the problem reduces to calculating the potential due to the source (I_0). This is most readily accomplished by assuming that in addition to (I_0) there exists an infinite number of images of I_0. It will be evident from the preceding problem (single layer problem) that the relative magnitudes of the current source and its electrical images

will depend on the values of the resistivities of the media in which the images are assumed to exist.

Analysis of the two layered media is discussed in detail in Chapter VI.
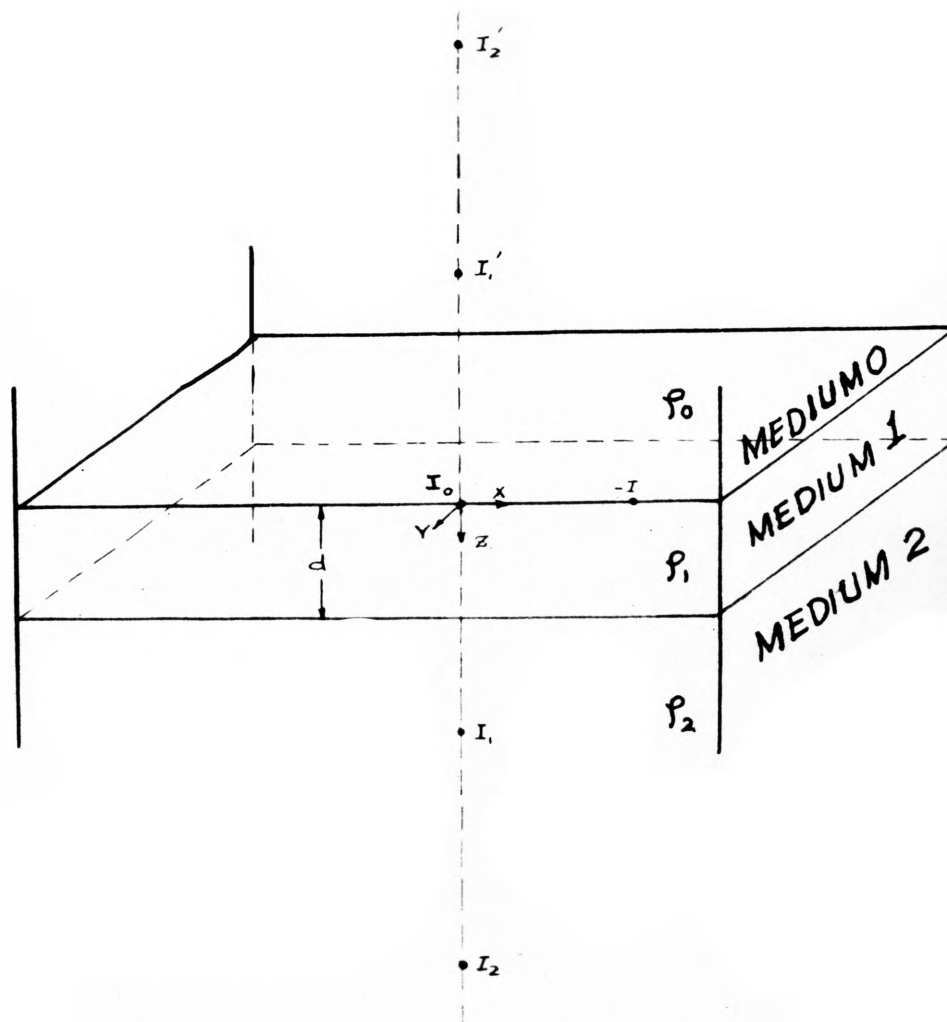
Fig. 2-3 Two-layer Problem and
Positions of Images

E.   Electrode Configurations.

Seven different electrode systems are widely used in field operations. Of these seven, described below, the first two are most frequently used.

(1) The Wenner-Gish-Rooney configuration has two potential electrodes placed in a line with the two current electrodes, so that the distances between the electrodes are equal. With (a) as the distance between the electrodes, the expressions for the configuration factor and the resistivity, from equation 1-2 and 1-4, are

$$F = a$$
$$\rho = 2\pi Ra \qquad\qquad 2\text{-}15$$

(2) The Lee Partitioning method is similar to the Wenner configuration, with an additional potential electrode provided halfway between P_1 and P_2. Two potential measurements are made, one for the left and another for the right interval.

$$F = 2a$$
$$\rho = 4\pi Ra \qquad\qquad 2\text{-}16$$

(3) The Asymmetrical Double Probe method has an electrode arrangement with the two potential electrodes placed asymmetrically between two current electrodes. The two potential electrodes are at distance (a) and (2a) from one current electrode. The other current electrode is at a much larger distance. If (l) is the distance between the current electrodes and (a) the potential-electrode interval, then

$$F = \frac{2a(l-a)(l-2a)}{(l-2a)^2 + al} \qquad\qquad 2\text{-}17$$
$$\rho = 2\pi R \; \frac{2a(l-a)(l-2a)}{(l-2a)^2 + al}$$

This equation will give the Wenner formula when $l = 3a$.

(4) The Asymmetrical Single Probe method results from the last (3) by using only one potential electrode at distance (a) from a current electrode and measuring the potential difference between this potential electrode and remote electrode. Then

$$F = \frac{a(1-a)}{(1-2a)} \qquad \text{2-18}$$

$$\rho = 2\pi R \frac{a(1-a)}{(1-2a)}$$

(5) The Double Equidistant Probe method is a modification of configuration (3). Potential electrodes are placed at (a) and (2a) from the first current electrode, and the second current electrode is far removed, i.e., C_2 is placed at infinity. Thus, $C_2P_1 = C_2P_2 = \infty$ and

$$F = 2a \qquad \text{2-19}$$

$$\rho = 4\pi Ra$$

(6) The Double Probe method with Unequal Probe Spacing differs from the last by an unequal electrode spacing and is generally used with potential electrodes in a line at right angles to the current electrode line. If $C_1P_1 = a$ and $C_1P_2 = b$, and C_2 is placed at infinity, then

$$F = \frac{ab}{b-a} \qquad \text{2-20}$$

$$\rho = 2\pi R \frac{ab}{(b-a)}$$

(7) The Single Probe method corresponds to configuration 4, with one current electrode at infinity. Potential difference is measured between the potential electrode and the other electrode. Because $C_2P_1 = C_2P_2 = \infty$, and $C_1P_1 = \infty$, $C_1P_2 = a$,

$$F = a \qquad \text{2-21}$$

$$\rho = 2\pi Ra$$

III. NEW CONFIGURATIONS

Two new electrode configurations are discussed in this chapter.
The electrode arrangement consists essentially of two pairs of
electrodes. The two electrodes in each pair have a fixed separation (a).
The distance between the two pairs is much larger than (a) and is
called the electrode pair separation (r). In the first configuration
one pair of electrodes is composed of two current electrodes and
the other pair is composed of two potential electrodes (see Figure 3-1).
In the second configuration each pair of electrodes is composed of
a current electrode and a potential electrode (see Figure 3-3).
For simplicity these two new configurations are called the A-config-
uration and the B-configuration.

A. The A-Configuration.

In this configuration, one electrode pair is composed of current
source electrode C_1 and sink electrode C_2 (see Figure 3-1), and the
other pair is composed of two potential electrodes P_1 and P_2.
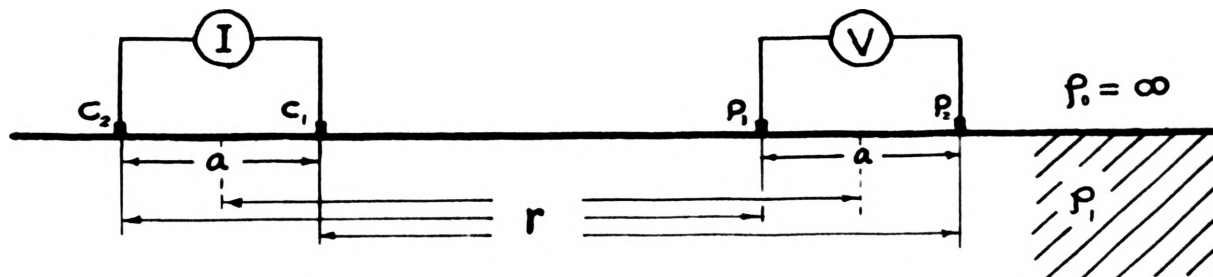
Fig. 3-1 The A-configuration and
Distance Relation

The resistivity of the earth measured by this configuration can be calculated from the potential difference between the two potential electrodes P_1 and P_2. To obtain a mathematical solution of the potential difference, the potential at a point is first derived.

If a potential electrode, not necessarily in a straight line with the current electrodes, is placed within a infinite homogeneous medium, Fig. 3-2, the potential V at the electrode P can be derived as follows.
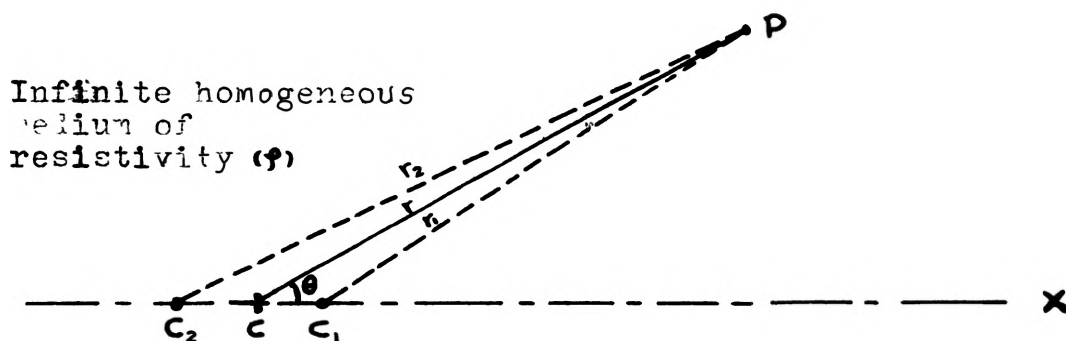
Fig. 3-2   An Electric Dipole in an
Infinite Homogeneous Medium

Let the distance

$$C_1 C_2 = a$$

$$P\ C_1 = r_1$$

$$P\ C_2 = r_2$$

$$\theta = \angle PCX \approx \angle PC_1X \approx \angle PC_2X$$

Let the distance from P to the point (C) located at the center of line C_1C_2, equal (r). The potential at P is, from equation 2-5

$$V_p = \frac{I\rho}{4\pi}\left(\frac{1}{r_1} - \frac{1}{r_2}\right) \qquad \text{3-1}$$

where I is the current flowing from C_1 to C_2, ρ is the resistivity of the medium.

$$r_1 = \left[r^2 + \left(\frac{a}{2}\right)^2 - ar\cos\theta\right]^{\frac{1}{2}} = r\left[1 + \left(\frac{a}{2r}\right)^2 - \frac{a}{r}\cos\theta\right]^{\frac{1}{2}}$$

$$r_2 = \left[r^2 + \left(\frac{a}{2}\right)^2 - ar\cos\theta\right]^{\frac{1}{2}} = r\left[1 + \left(\frac{a}{2r}\right)^2 + \frac{a}{r}\cos\theta\right]^{\frac{1}{2}} \qquad \text{3-2}$$

When $r \gg a$,

$\left(\frac{a}{2r}\right)^2$ is so small that the value is negligible.

Therefore—

$$r_1 = r\left[1 - \frac{a}{r}\cos\theta\right]^{\frac{1}{2}} \qquad \text{3-2a}$$

$$r_2 = r\left[1 + \frac{a}{r}\cos\theta\right]^{\frac{1}{2}}$$

and

$$V_p = \frac{I\rho}{4\pi}\left\{\frac{1}{r(1 - \frac{a}{r}\cos\theta)^{\frac{1}{2}}} - \frac{1}{r(1 + \frac{a}{r}\cos\theta)^{\frac{1}{2}}}\right\} \qquad \text{3-1a}$$

From the binomial theorem:

$$(x+y)^n = x^n + nx^{n-1} + \frac{n\cdot(n-1)}{1\cdot 2}x^{n-2}y^2 + \frac{n(n-1)(n-2)}{1\cdot 2\cdot 3}x^{n-3}y^3 \cdots$$

so that

$$\left(1 - \frac{a}{r}\cos\theta\right)^{-\frac{1}{2}} = 1 + \frac{1}{2}(1)^{-\frac{3}{2}}\frac{a}{r}\cos\theta + \frac{(-\frac{1}{2})(\frac{1}{2})}{1\cdot 2}(1)^{-\frac{5}{2}}\left(\frac{a}{r}\cos\theta\right)^2 \cdots \qquad \text{3-2b}$$

$$\left(1 + \frac{a}{r}\cos\theta\right) = 1 - \frac{1}{2}(1)^{-\frac{3}{2}}\frac{a}{r}\cos\theta + \frac{(-\frac{1}{2})(\frac{1}{2})}{1\cdot 2}(1)^{-\frac{5}{2}}\left(\frac{a}{r}\cos\theta\right)^2 \cdots$$

The odd terms will cancel when subtracted. The fourth and higher

terms contain powers of $\frac{a}{r}$ Cosθ which are negligibly small. Therefore:

$$V_p = \frac{I\rho}{4\pi}\left(\frac{1}{r}\right)\left(1 + \frac{a}{2r}\text{Cos}\theta - 1 + \frac{a}{2r}\text{Cos}\theta + \ldots \right)$$

$$\approx \frac{I\rho}{4\pi}\left(\frac{1}{r}\right)\left(\frac{2a}{2r}\text{Cos}\theta\right)$$

$$= \frac{I\rho}{4\pi}\quad \frac{a\text{Cos}\theta}{r^2} \tag{3-1c}$$

When used for electrical resistivity surveying, the electrodes are usually arranged in a straight line. Therefore, for this special case

$$\theta = 0, \quad \cos\theta = 1$$

When the electrodes are all placed on the earth's surface, the current flux in the conducting medium is doubled (see Single Layer Problem, Ch. 2). The resistivity of the air, ρ_0, is taken as infinite; the resistivity of the earth is ρ_1. Therefore for the semi-infinite homogeneous medium

$$V_p = \frac{I\rho_1}{2\pi}\quad \frac{a}{r^2} \tag{3-3}$$

We can consider the two current electrodes as a point C which has the current strength (Ia), and a distance r from the point P. The value of potential at P, due to current Ia at C, is inversely proportional to the square of distance (r).

As illustrated in Fig. 3-1, the distance from the middle of C_1C_2 to the middle of P_1P_2 is (r), and each electrode separation within pairs is (a) so that

$$P_1C = r - \frac{a}{2}$$

$$P_2C = r + \frac{a}{2}$$

Thus the potential at each potential electrode is:

$$V_1 = \frac{I \rho_i \cdot a}{2\pi} \left[\frac{1}{(r-\frac{a}{2})^2} \right]$$

$$V_2 = \frac{I \rho_i \cdot a}{2\pi} \left[\frac{1}{(r+\frac{a}{2})^2} \right]$$

and the potential difference between P_1 and P_2 is:

$$\Delta V = V_1 - V_2$$

$$= \frac{(Ia)\rho_i}{2\pi} \left[\frac{1}{(r - \frac{a}{2})^2} - \frac{1}{(r + \frac{a}{2})^2} \right]$$

$$= \frac{Ia \cdot \rho_i}{2\pi} \left[\frac{1}{r^2 + \frac{a^2}{4} - ar} - \frac{1}{r^2 + \frac{a^2}{4} + ar} \right]$$

Relative to r^2,

$\frac{a^2}{4}$ is so small that the value is negligible.

therefore,

$$\Delta V \approx \frac{Ia \rho_i}{2\pi} \left[\frac{1}{r^2 - ar} - \frac{1}{r^2 + ar} \right]$$

$$= \frac{Ia \cdot \rho}{2\pi} \left(\frac{1}{r}\right)\left[\frac{1}{r-a} - \frac{1}{r+a} \right]$$

$$= \frac{Ia \rho_i}{2\pi} \left(\frac{1}{r}\right)\left(\frac{2a}{r^2 - a^2} \right)$$

$$= \frac{I \rho_i}{2\pi} \frac{2a^2}{r(r^2 - a^2)} \qquad\qquad 3\text{-}4$$

if $r > a$, $r^3 \gg ra^2$, therefore

$$\Delta V \approx \frac{I \rho_i}{2\pi} \frac{2a^2}{r^3} \qquad\qquad 3\text{-}4a$$

The resistivity of the earth ρ_i can be derived from this equation.

$$\rho_i = \frac{\Delta V}{I} 2\pi \left[\frac{r(r^2 - a^2)}{2a^2} \right] \qquad\qquad 3\text{-}5$$

or from (3-4a)

$$\rho_1 = \frac{2\pi}{I} (\Delta V) \left(\frac{r^3}{2a^2}\right) \qquad \text{3-5a}$$

The above solution is applicable at any point in line with the current electrodes in the medium. It is similar to the potential of an electric dipole (HARNWELL; SMYTHE, 1950). The dipole solution for potential is often used in oil well lateral type resistivity logging. For surface resistivity measurement however, this solution can be obtained as follows:

Refer to Figure 3-1.

$$V_1 = \frac{I\rho_1}{2\pi} \left(\frac{1}{r-a} - \frac{1}{r}\right) = \frac{I\rho_1}{2\pi} \frac{a}{r(r-a)}$$

$$V_2 = \frac{I\rho_1}{2\pi} \left(\frac{1}{r} - \frac{1}{r+a}\right) = \frac{I\rho_1}{2\pi} \frac{a}{r(r+a)}$$

Therefore

$$\Delta V = \frac{I\rho_1}{2\pi} \left[\frac{1}{r-a} - \frac{1}{r+a}\right] \frac{a}{r} = \frac{I\rho_1}{2\pi} \left[\frac{2a^2}{r(r^2-a^2)}\right]$$

$$\rho_1 = 2\pi \frac{\Delta V}{I} \cdot \frac{r(r^2-a^2)}{2a^2} \qquad \text{3-5}$$

when $r \gg a$;

$$\rho_1 \approx 2\pi \frac{\Delta V}{I} \frac{r^3}{2a^2} \qquad \text{3-5a}$$

B.   The B-Configuration.

In this configuration, a potential electrode P_1 is placed a distance (a) apart from the current source C_1, and the other potential electrode P_2 is a distance (a) from current sink C_2. These two pairs are placed a distance (r) apart. For simplicity assume the electrodes are all on the earth's surface (Fig. 3-3).
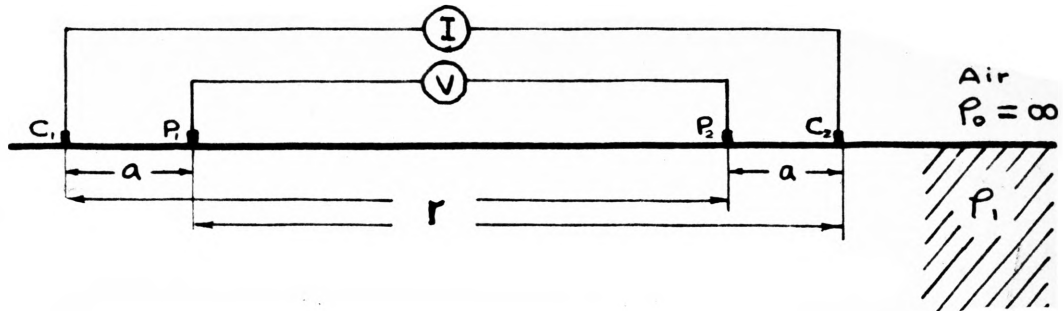
Fig. 3-3 The B-configuration
            and Distance Relation

$$V_1 = \frac{I\rho_1}{2\pi}\left(\frac{1}{a}-\frac{1}{r}\right) = \frac{I\rho_1}{2\pi}\left(\frac{r-a}{ar}\right)$$

$$V_2 = \frac{I\rho_1}{2\pi}\left(\frac{1}{r}-\frac{1}{a}\right) = \frac{I\rho_1}{2\pi}\left(\frac{a-r}{ar}\right)$$

3-6

$$\Delta V = V_1 - V_2$$

$$= \frac{I\rho_1}{2\pi}\left[\frac{2(r-a)}{ar}\right]$$

3-7

so that

$$\rho_1 = \frac{2\pi}{I}(\Delta V)\left(\frac{ar}{2(r-a)}\right)$$

3-8

If $r \gg a$, then $\frac{r}{r-a} \approx 1$

and

$$\rho_1 = \frac{\pi a}{I}\Delta V$$

3-8a

In the field operation, if we adjust the current flow so that $\frac{\pi a}{I}$ or, more accurately, $\frac{\pi a}{I}\left(\frac{r}{r-a}\right)$ is an integer, then the

resistivity value may be obtained directly by multiplying the $\triangle V$ reading by that integer.

If $r = 2a$, this configuration will become the Wenner configuration.

In lateral devices of cil well resistivity surveys, the distance relation is the reverse of B-configuration. In lateral device the distance (a) is extended so that $a \approx r$. If we let

$$R = a + (r-a) = r$$

$$A = r-a \qquad \text{(See Fig. 3-4)}$$
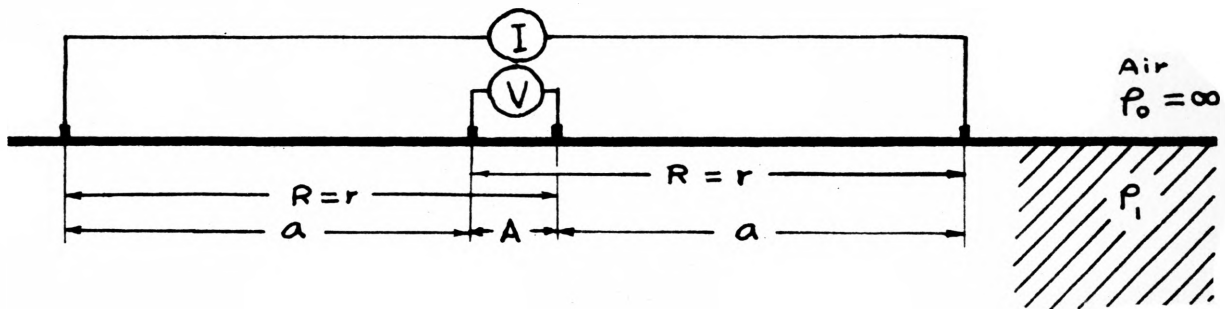
Fig. 3-4 The Modified B-configuration

Then the equation for lateral resistivity can be obtained as follows:

$$V_1 = \frac{I\rho_i}{2\pi}\left[\frac{1}{R-A} - \frac{1}{R}\right] = \frac{I\rho_i}{2\pi}\left[\frac{A}{R(R-A)}\right]$$

$$V_2 = \frac{I\rho_i}{2\pi}\left[\frac{1}{R} - \frac{1}{R-A}\right] = \frac{I\rho_i}{2\pi}\left[\frac{-A}{R(R-A)}\right]$$

$$\triangle V = V_1 - V_2$$

$$= \frac{I\rho_i}{\pi}\left[\frac{A}{R(R-A)}\right]$$

3-9

This equation can also be obtained directly from equation 3-7.

$$\Delta V = \frac{I\rho}{2\pi}\left[\frac{2(r-a)}{ar}\right] \tag{3-7}$$

$$= \frac{I\rho}{2\pi}\left[\frac{2A}{R(R-A)}\right]$$

$$\rho = \frac{2\pi}{I}\Delta V\left[\frac{R(R-A)}{2A}\right] \tag{3-10}$$

If we let $\quad \dfrac{R(R-A)}{2A} = F \quad$ then $\quad \rho = 2\pi \cdot F \cdot \dfrac{\Delta V}{I}$

$$\tag{3-10a}$$

Thus the resistivity ρ can be obtained from the potential difference ΔV by multiplying by a constant. This completes the derivation of resistivity equations and configuration factors for both of the new configurations.

IV. APPLICATION OF NEW CONFIGURATIONS TO DEPTH PROBING AND LATERAL TRAVERSING

The interpretation of experimental resistivity results is based on the measurement of apparent resistivity, (ρ_a). The apparent resistivity can be generalized by the equation

$$\rho_a = 2\pi RF \qquad\qquad 1\text{-}2$$

where

$$R = \frac{\Delta V}{I} \qquad\qquad 1\text{-}3$$

and

$$1/F = \left[\frac{1}{c_1 p_1} - \frac{1}{c_2 p_1} - \frac{1}{c_1 p_2} + \frac{1}{c_2 p_2} \right] \qquad\qquad 1\text{-}4$$

(R) is called the configuration resistance and (F) the configuration factor. (See Fig. 4-1).
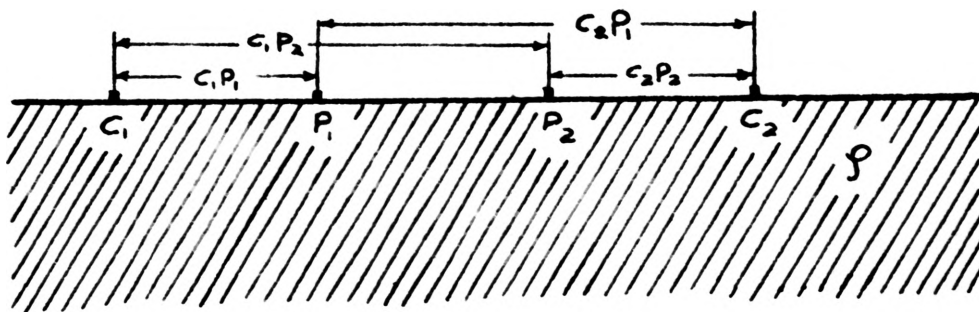
Fig. 4-1 Distance relation of Electrode Configuration in Resistivity Method

The value of the apparent resistivity obtained from this equation is governed by the position of the electrodes and the distribution of resistivity within the earth. It is the aim of the resistivity method to determine the true earth resistivity distribution by

measuring the variation of apparent resistivity with variation of the arrangement and spacing of electrodes.

Certain simplifying assumptions are often made about the types of resistivity distributions which occur in practice. Theoretical resistivity curves are obtained by calculating the resistivity values under such assumptions. Comparison of theoretical curves and field resistivity curves will often times give important information concerning the subsurface structure. A common example among such assumptions is the two horizontal layer problem.

Two general approaches are used for taking resistivity measurements in the field. With the first, the center of the electrode spread remains fixed but the spacing of electrodes is progressively increased until the maximum desired depth of penetration is reached. This method locates horizontal discontinuities in conductivity and makes it possible to determine their depths. The name depth probing, or vertical profiling is given to this method. In the second type of measurement the electrode spacings are fixed and the array of electrodes is moved with constant spacing from one place to another. The values of apparent resistivity are plotted at the midpoints. Data are contoured or profiled over the area of interest. This method is called lateral resistivity traversing, or horizontal profiling.

A. Depth Probe Method.

The quantitative interpretation of resistivity data has been the subject of mathematical studies for many years. Numerous papers about this subject have appeared in the geophysical literature. However,

in spite of the attention that has been given to the problem, it is very difficult to obtain reliable results by applying theoretical analysis to resistivity data obtained in the field. This is because the theory thus far worked out can only be applied to simple models, such as multiple layers (up to four) separated by plane, preferably parallel, interfaces. It is seldom that the rock formations near the earth's surface exhibit such a simple stratification in electrical properties. The variations in resistivity are usually much more complex both in the lateral and vertical directions.

Local resistivity variations can be tested by traversing along the line of the probe using a constant electrode spacing or by running probe lines in different azimuths keeping their centre points fixed (HUBBERT, 1934). Unfortunately these methods are very time consuming and are rarely employed in the field. As a possible alternative to the above procedures, a method has recently been described by CARPENTER (1955) whereby three resistances are measured for each separate electrode spacing.

B. Lateral Traversing Method.

Lateral traverse investigations are usually conducted to determine lateral variations associated with fault zones, contacts of different formations, variation in depth to formerly determined beds, etc. Lateral resistivity measurements are often termed "constant depth" traverses, horizontal profiling, traversing method, or electrical trenching. Measurements are carried out, as the terms indicate, by moving the electrode configuration with the fixed electrode

spacing (a) as a unit along a traverse line that crossed the area.
The line of electrode configuration is generally either along or
perpendicular to the traverse line. Variations in resistivity are
plotted against the traverse distance. The measurements can be summar-
ized or represented in the form of profiles or maps of resistivity,
according to circumstances. These are comparable to the geological
cross sections and maps prepared by the geologist.

This method can be used very well for the location of local bodies
of contrasting resistivity, especially if these bodies are near the
surface. The interpretation of resistivity data obtained by this
method is difficult because there are many factors affecting the
magnitude and variation of measured resistivity values. The amount of
change will depend mainly upon (1) electrode configuration, (2) relative
resistivities of the local body and the surrounding rock, and (3) the
size and depth of the body. More detailed discussion of the lateral
traversing method is presented in Chapter VI.

C. Theoretical Consideration.

From the viewpoint of field survey, time consumption is an
important aspect of the electrical resistivity work. The developement
of continuous resistivity measuring methods will of course simplify
the work and reduce time consumption. Also, this develop ment would
make it possible to apply horizontal traverse, depth probe, local
resistivity determination and other techniques to a whole area, or
any special spot in the area of exploration, within a short time. A
method and apparatus for continuous electrical exploration was invented

and patented by J. J. Jakosky. However, the Jakosky method has not been widely used in field survey. It may be possible that application or adaptation of A-configuration or B-configuration to the Jakosky method will develop a quick and dependable method for electrical resistivity surveying.

It is clear, from equation 1-2, that the apparent resistivity measurement is dependent upon the configuration resistance, (R), and the configuration factor, (F). (R) varies with the resistivity of the earth and with electrode spacing. (F) is a fuction of electrode spacing. When a four-electrode configuration is applied to depth probing of a homogeneous medium, the value of (F) is inversely proportional to the value of (R) in a semi-infinite homogeneous and isotropic medium where the resistivity (ρ) is constant. According to equation 1-2,

$$\rho = 2\pi RF \qquad\qquad 1\text{-}2$$

If we solve for (R), then

$$R = \frac{\rho}{2\pi F} \qquad\qquad 4\text{-}1$$

where, from equations 3-4 and 3-8, the value of (F) is

$$F_A = \frac{r(r^2 - a^2)}{2a^2} \qquad \text{for A-configuration} \qquad 4\text{-}2$$

$$F_B = \frac{ar}{2(r-a)} \qquad \text{for B-configuration} \qquad 4\text{-}3$$

For a constant earth restivity value, (R) will be inversely proportional to the value of (F). If we substitute the equation for (F) into equation 4-1, the variation of (R) with increase of electrode pair separation (r) will be obtained.

Tables 4-1 and 4-2 are the variation of (F) for respectively, A-configuration and B-configuration with increase of (r) expressed in units of (a). This variation can be shown graphically. Figures 4-2 and 4-3 show the variation of (F) plotted from the data in Tables 4-1 and 4-2.

D.   A-Configuration.

From equations 1-2 and 4-2, Table 4-1, and Fig. 4-2, it can be seen that the measurement of earth resistivity is very sensitive to the electrode pair separation (r) for the A-configuration. The value of (F) increases rapidly with increase of electrode pair separation, (r). Assuming the resistivity of the earth is not changed, (R) will become very small and rather difficult to determine accurately. For example, assume that measurements were taken over an infinite homogeneous medium of resistivity 5×10^5 ohm-cm, with constant electrode spacing (a) of 100 cm, and electrode pair separation (r) increasing in units of (a). From equations 1-2 and 3-5 for constant resistivity (ρ), the configuration resistance (R) which will be measured from instruments is inversely proportional to the configuration factor (F). The variation of (F), and of (R) which would be measured at the instruments, is calculated and tabulated in Table 4-3.

In this example, the assumed resistivity value of the earth, 5×10^5 ohm-cm, is not an extreme value for common rocks. This example also illustrates how deep the A-configuration can measure before instrumental difficulties occur. A mathematical

TABLE 4-1

Variation of (F) with increase of (r)
A-Configuration $\quad F_A = \dfrac{r(r^2 - a^2)}{2a^2}$

r/a	F/a (cm)
1	0
2	3
3	12
4	30
5	60
6	105
7	168
8	252
9	360
10	495
11	660
12	858
13	1092
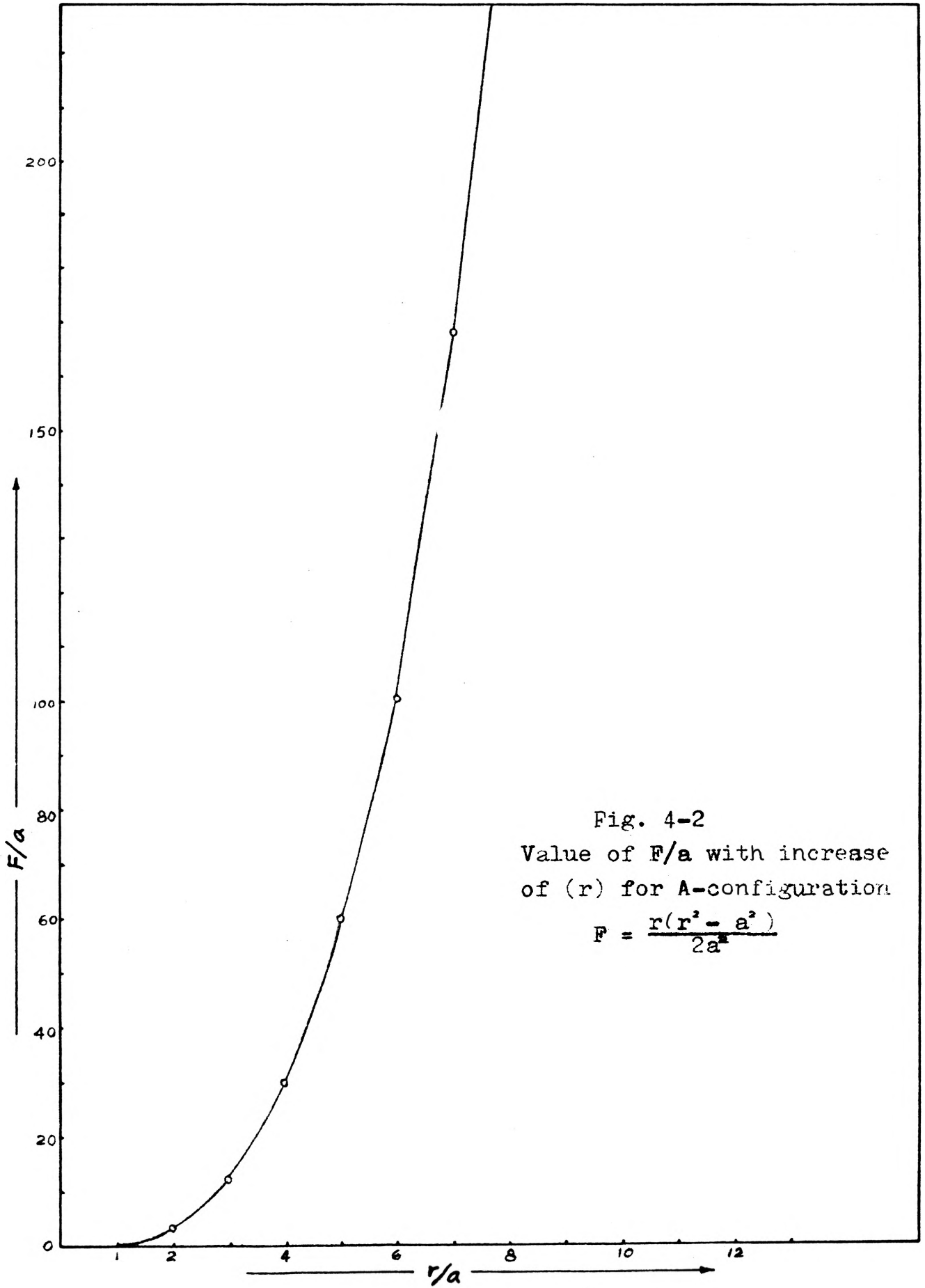
Fig. 4-2
Value of **F/a** with increase
of (r) for **A**-configuration

$$F = \frac{r(r^2 - a^2)}{2a^2}$$

TABLE 4-2

Variation of (F) with Increase of (r)

B—Configuration $F_B = \dfrac{ar}{2(r-a)}$

r/a	(r-a)/a	F/a (cm)
1	0	
2	1	1
3	2	0.75
4	3	0.66
5	4	0.625
6	5	0.600
7	6	0.583
8	7	0.571
9	8	0.562
10	9	0.556
11	10	0.550
12	11	0.546
14	13	0.538
16	15	0.533
20	19	0.526

Fig. 4-3 Value of F/a with
          increase of (r) for
          B-configuration

$$F = \frac{ar}{2(r - a)}$$
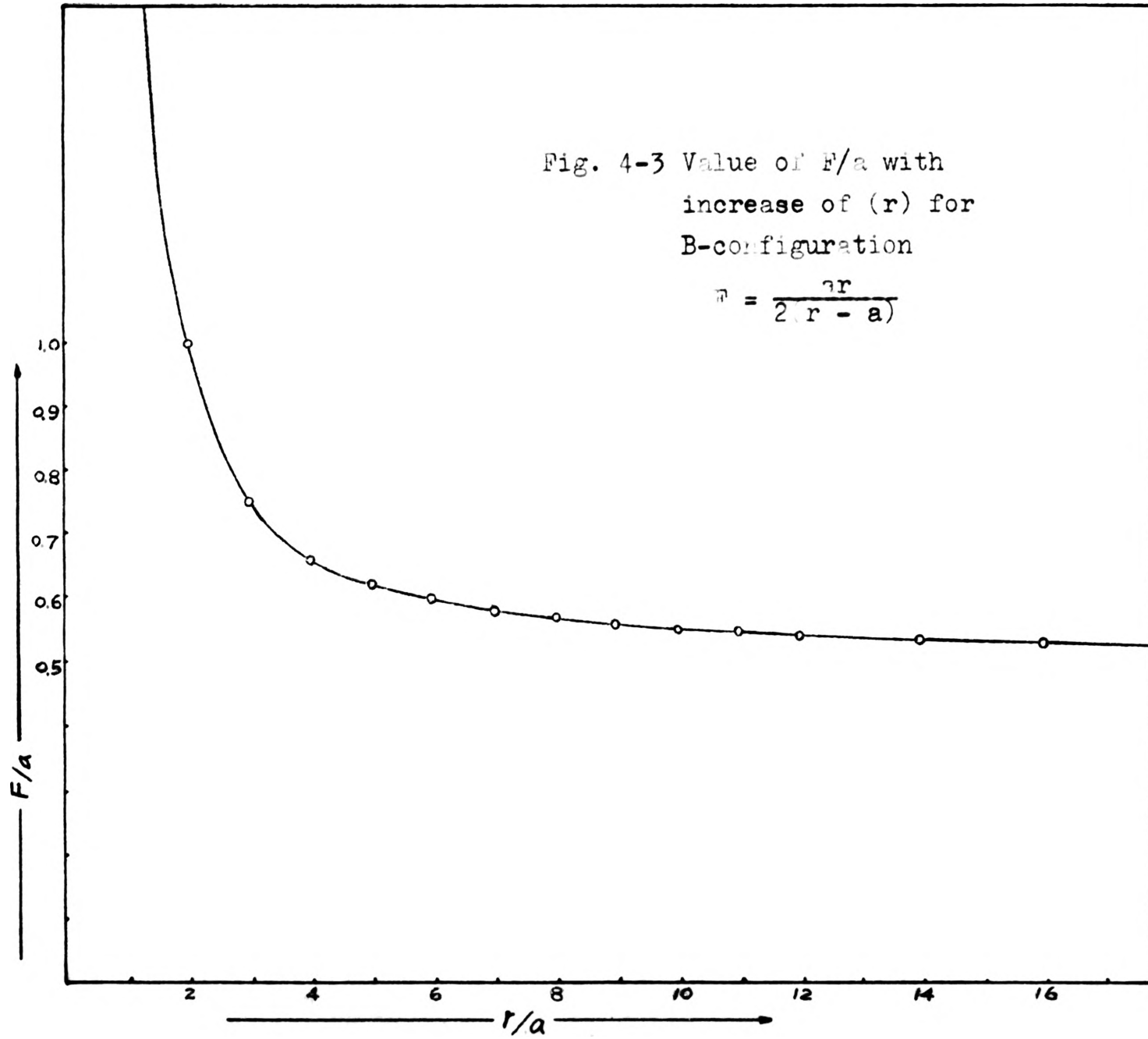
TABLE 4-3

Change of (F) and (R) with the Increase of Electrode Pair Separation over an Infinite Homogeneous Medium

(Assume that $\rho = 5 \times 10^5$ ohm-cm)

Electrode Pair Separation r (cm)	Configuration Factor F (cm)	Configuration Resistance R(ohm)
1	0	
2	3	2.563×10^2
3	12	6.632×10
4	30	2.653×10
5	60	1.326×10
6	105	7.579
7	168	4.737
8	252	3.158
9	360	2.211
10	495	1.608
11	660	1.206
12	858	9.275×10^{-1}
13	1092	7.288×10^{-1}
14	1365	5.830×10^{-1}
15	1680	4.737×10^{-1}
16	2040	3.901×10^{-1}
17	2448	3.251×10^{-1}
18	2907	2.738×10^{-1}
19	3420	2.327×10^{-1}
20	3990	1.994×10^{-1}
21	4620	1.723×10^{-1}
22	5313	1.498×10^{-1}
23	6072	1.311×10^{-1}
24	6900	1.153×10^{-1}
25	7800	1.020×10^{-1}
26	8775	9.069×10^{-2}
27	9828	8.097×10^{-2}
28	10962	7.260×10^{-2}
29	12180	6.534×10^{-2}
30	13485	5.901×10^{-2}

analysis of the depth of penetration of Wenner configuration was published by H. M. Evjan (1938). It is usually stated that the depth of penetration of the Wenner configuration is approximately equal to its electrode spacing (a). No mathematical analysis for the depth of penetration of the A-configuration has been done. However, it is clear from Fig. 3-1 that the depth of penetration of the A-configuration is less than the total configuration distance, (r+a). Instrumentally, the reading of (R) for the A-configuration will be fairly difficult, in this example, if the depth probe is expanded to r = 12a. The value of (R) will decrease to such a small value that any change in resistivity due to inhomogeneity of the earth, or two layer or three layered media, or any other changes in the earth-resistivity, will be concealed in this very low value of (R). If the electrode pair separation (r) is expanded further, the reading will be even more difficult. It is rather difficult to state a critical distance for a depth probe survey. If r = 12a is close to the instrumental limit, the depth of penetration will be less than about 13 meters for the above example. This value of depth probing is not satisfactory for general geophysical surveying. For a depth probing method, a depth of several hundred feet is usually desired. If the A-configuration is applied to depth probing, very accurate devices for measuring the current and the voltage difference, as well as accurate electrode pair separation measurement, will be required.

The greatest advantage in this configuration is that if a continuous resistivity survey is done in an area, either depth probing or horizontal profiling method, it is not necessary to connect

the vehicle which carries the current electrode pair to the vehicle which carries the potential electrode pair. The values of (I) and (ΔV) can be obtained separately in the respective vehicles. Separate measurement of potential and current in two vehicles may eliminate inductive effects on a precision meter.

E. B-Configuration.

From equations 1-4 and 3-8, the configuration factor, (F) will become

$$F = \frac{ar}{2(r-a)}$$

From this equation it can be seen that (F) approaches $a/2$ as the electrode pair separation (r) increases. It is also apparent that (F) is proportional to approximately the first power of (a) when (r) is large. Therefore, in field operations, small inaccuracy of the measurement of (a) when (r) is much greater than (a) does not cause a very large error in the value of apparent resistivity. This property is very important and helpful when the work is applied to an area where topography is rather rough and accurate measurement of the separation distance is rather difficult. If the A-configuration is applied to such areas of rough terrain, error caused by incorrect distance measurement is more difficult to avoid.

Another important property of the B-configuration, according to equation 3-8, is that the reading of configuration resistance (R) approaches a value of $\rho/\pi a$ as the distance (r) increases, because the configuration factor (F) approaches $a/2$. Thus, for large values

of (r), the B-configuration is more sensitive to changes in the earth resistivity than is the A-configuration. The B-configuration may be more useful for detecting small change in earth resistivity such as caused by a vertical discontinuity, a horizontal discontinuity, a change in the dip of the subsurface layer, or change in the earth resistivity due to anisotropy of the medium. These changes in earth resistivity will more strongly affect the value of instrumentally measured value, (R).

Difficulty with the B-configuration will occur when a survey traverses a highly resistive rock. Consequently the measured voltage drop V will be very high and the current (I) will be small. However, this is a common difficulty of the electrical resistivity survey, no matter what configuration is applied. For the Wenner configuration, where

$$R_{Wenner} = \frac{\rho}{2\pi F} = \frac{\rho}{2\pi a}$$

(R_{Wenner}) will decrease with increase of (a). In the B-configuration (R_B) will increase with increase of electrode pair separation (r) and (R_B) will approach the value of $\rho/\pi a$, or ρ/π where (a) is unity. On the other hand, a continuous resistivity survey for depth probe method by using the B-configuration can be applied to the field survey by two vehicles where four vehicles are required if the Wenner configuration is applied. Only the value (r) increases for the B-configuration.

For the Wenner configuration, all electrode spacings (a) must be changed. Therefore, from the viewpoint of field operation, operation cost, error in distance measurement, operation time, sensitivity, and accuracy will be superior for the B-configuration compared to the Wenner configuration.

F.   Effect of Earth Current.

In the area of survey, earth current may be developed by
electro-chemical action between minerals and the solutions with which
they are in contact. When the A-configuration is applied to the
field, the potential difference due to earth current may be even
larger than the potential difference due to the applied current.

When the Wenner configuration is applied to the field, the
effect of earth current can be removed by reversing the direction of
applied current. The two readings are averaged. This technique is
also applicable to the A-configuration and B-configuration.

G.   Conclusions.

Applying either the A- or B-configuration to both depth probing
and lateral resistivity traversing methods seems to present no
particular difficulty. If the A-configuration is applied, precise
distance measurement and precise instruments are required. In the
depth probe method, the electrode pair separation (r) is expanded
in units of (a). In the lateral traversing method, the electrode
configuration is carried as a unit along the line of traverse. The
distance relation is constant and also the depth of penetration. It
should be noted that the electrode positions changed with each measure-
ment in both methods. This characteristic shows that the mobility
of the electrodes will greatly affect the ease of the field operation.
If Jakosky's continuous resistivity surveying method is applied to
the field, A-configuration and B-configuration are more economical
and easier to apply than the Wenner configuration.

V. NEW CONFIGURATIONS APPLIED TO LATERAL TRAVERSING
OF A VERTICAL DISCONTINUITY

Lateral resistivity investigations are usually conducted to determine lateral variations of earth resistivity such as those associated with fault zones, contacts of different formations, or variation in depth to beds previously measured by depth probing. Lateral resistivity measurements are carried out by moving the electrode configuration as a whole, without changing electrode spacing, along a traverse line in the area of survey. This method is also termed "constant depth" traverse, horizontal profiling method, traversing method, or electrical trenching method. Traverse lines are chosen either along the line of configuration, or perpendicular to it. Measured resistivity values are generally plotted against the traverse distance. Each resistivity value is plotted at the center point of the electrode configuration. The results can be summarized in the form of profiles or as maps of resistivity, according to circumstances. These profiles or maps are comparable to the geological cross sections and maps prepared by the geologist. Sometimes double-depth measurements, in which two measurements are made at each location with different electrode spacings, will be taken of the area of survey. The differentiation of "near-surface effects" from "deeper structural effects" can often times be accomplished by comparing results of two different electrode spacing, i.e., two different depth of penetration. Resistivity profiles of two different spacings will give more information for comparison with the geologic cross sections. It is clear that the lateral traversing method can be used more successfully for subsurface

structure surveying when the geologic conditions of the area are well known.

Interpretation of resistivity data obtained by lateral investigations requires consideration of many factors which cause variations of the measured resistivity. These factors include electrode configuration, relative resistivities of the affecting body and the surrounding rock, size, shape, and depth of the body. Certain assumptions can often be made about the types of resistivity distributions which are found in practice. Based on these assumptions, theoretical curves of apparent resistivity can be computed. Common simplifying assumptions made to calculate these theoretical curves are that fault planes are vertical, or that dipping beds or dipping fault planes have constant dip, and that buried bodies have simple geometric shapes. Within limits imposed by these assumptions, valuable information concerning the actual survey results can sometimes be obtained by comparing the theoretical resistivity curves with the measured curves.

Many papers have been published during the past thirty years presenting solutions to the simplified problems. There have been two groups of workers, the so called "image school" and the "harmonic school" respectively, who have attacked the problem of interpretation of resistivity data under assumptions of simplified geologic conditions.

Solutions of the "image school" are based upon Maxwell's theory of images. The potential at a point in a medium is expressed as that due to current flow from current electrodes and their "images". The current from the images is actually current "reflected" from formation boundaries. The image solution is not an exact solution. The current

distribution is not uniform in all directions if a discontinuity of
the medium exists near the electrodes. In the image theory, solutions
can only be considered analogous to the reflections of light from a
mirror; there is no way to consider the distortion of current distri-
bution due to a boundary. However, deviation of calculated values
from exact values is often times very small. The mathematics is
relatively simple and equations are expressed as summations of potential
due to current electrodes and their images. Therefore this method
of solution is still widely used.

Tagg (1930) was the first who applied the method of images to
obtain resistivity curves for the Wenner configuration traversing
over a vertical fault plane. The first image solution for resistivity
values over a dipping bed, based on the Wenner configuration, was made
by Aldredge (1933). A number of papers extending Aldredge's work
has been published. However, for a dipping bed problem, the image
method has a certain limit of accuracy and application (UNZ, 1953;
MAEDA, 1955). Image method is applicable when electrodes are all in
the upper medium, but not when the configuration crosses the contact,
nor when the electrodes are in the underlying medium. When a boundary
of earth media is parallel to the surface of the earth, an exact
solutions requires the sum of potentials due to an infinite number of
images reflected at the boundary. An example is given in Chapter VI.
Image theory applied to a dipping bed problem is valid only when the
dip angle is a submultiple of π if the bottom layer is perfectly in-
sulating, or a submultiple of $\pi/2$ if the bottom layer is perfectly
conductive. If the reflection factor (k) is other than (+1) or (-1),

the image method is not strictly applicable, but the deviations caused by this distortion are negligible for small absolute values of the reflection factor (k) and also for small dip angles. A detailed discussion was made by M. Unz (1953).

A special case in the dipping bed problem occurs when the boundary plane is vertical. Solution across the boundary can be obtained by image method for this case.

To summarize, image solutions are dependable only when applied to horizontal parallel layers (described in Chapter VI) or to a vertical fault plane. For the dipping bed problem, Aldredge s solution is close to an exact solution for a limited number of dip angles.

The harmonic school had an early start in the field of potential theory, solving potential distribution across a boundary of different media. It has a wide application to gravimetric and magnetic intensity problems, seismic wave propagation, and electrical potential distribution. It has given ever-increasing help in the solution of many geophysical problems. The equations of potentials are obtained by solving the Bessel's functions. Several harmonic solutions for the Wenner configuration, traversing over a dipping layer, (SKALASKAYA, 1948; MAEDA, 1955) or over a buried hemisphere, (COOK, 1954) have been published. The mathematics involved is difficult compared with that used in the image method solution.

A. Image Solution for Vertical Fault Plane Problem by Applying New Configurations.

The image method can be applied to solve for the resistivity of new configurations traversing across a fault plane. Solutions for the A-configuration

and the B-configuration traversing over a vertical fault plane are given here.

When a four-electrode system is moved as a whole perpendicularly toward the fault line, five possible positions of the electrodes in reference to the fault plane are obtained. These five cases are: (1) all electrodes in the first medium; (2) only one electrode across the fault plane; (3) two electrodes in each medium; (4) three electrodes in second medium; (5) all electrodes in the second medium. Each case should be considered independently. Equations for the new configurations are solved for each of these five electrode positions with respect to the fault plane. Each of the electrode positions is illustrated by figures in each case.

The calculated resistivity values are plotted at the center of the electrode configuration. The resistivity equations are expressed in terms of electrode spacing and distance (d) from the fault plane to the center of configuration.

According to the theory of images, the images must be considered when current electrodes and a potential electrode are inside the same medium. When they are in opposite sides of the fault plane, a fraction of the current (kI) will be reflected at the fault plane. So the effect due to a current electrode in the other medium is only $(1-k)I$. No image is considered in this case.

B. Solutions for A-Configuration.

1. Four electrodes in one medium (see Fig. 6-1).

For this solution the four electrodes are assumed to be in one medium of resistivity (ρ_1), separated by a vertical discontinuity

from a second medium of resistivity (ρ_2). The distance (d) from the center of the configuration to the fault plane is larger than half of the total electrode spacing $(d > \frac{r+a}{2})$, (a) is the constant electrode spacing, and (r) is the electrode pair separation. The source of current (I) is located at (C_1) and sink (-I) is located at (C_2). The potential values at each potential electrodes, (P_1) and (P_2), will depend upon the current strength of (I), of (-I), and of their images at (C_1') and (C_2') resulting from reflection on the fault plane.
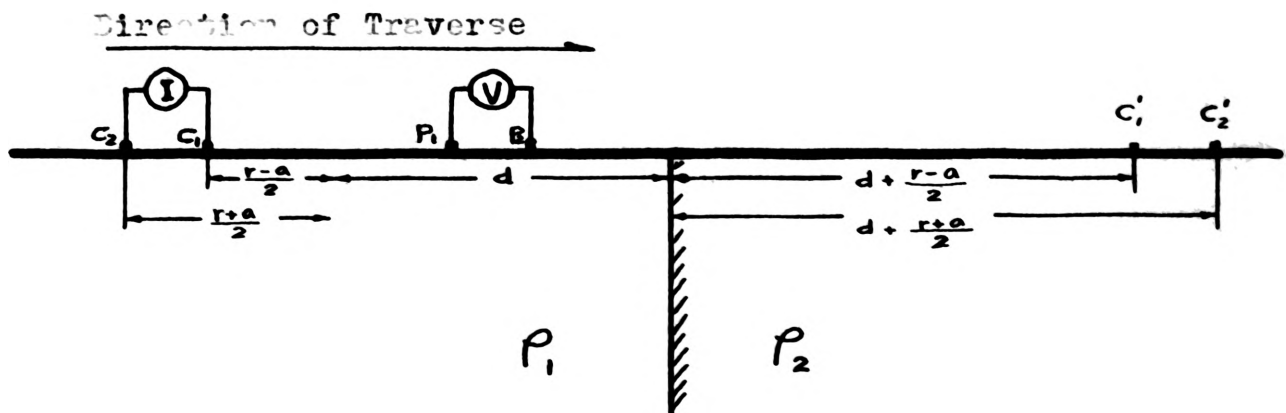

Fig. 5-1 Case 1, A-configuration: All Electrodes In The First Medium

The potential at (P_1) due to the source (I) at (C_1) is $\frac{I\rho}{2\pi} \left(\frac{1}{r-a} \right)$, and the potential at the same point (P_1) due to the sink (-I) at (C_2) is $\frac{-I\rho}{2\pi} \left(\frac{1}{r} \right)$. The potential resulting from the image

at (C_1') is

$$\frac{I\rho_1}{2\pi}\left(\frac{k}{C_1'P_1}\right) = \frac{I\rho_1}{2\pi}\left[\frac{k}{\frac{r-a}{2}+d+d-\frac{r-a}{2}}\right] = \frac{I\rho_1}{2\pi}\left(\frac{k}{2d}\right)$$

Similarly, the potential due to the image of $(-I)$ at (C_2')

is $\frac{I\rho_1}{2\pi}\left(\frac{k}{2d+a}\right)$ where $k = (\rho_2-\rho_1)/(\rho_2+\rho_1)$ (see Equation 2-8).

The total potential at (P_1) is therefore

$$V_1 = \frac{I\rho_1}{2\pi}\left[\left(\frac{1}{r-a}-\frac{1}{r}\right)+k\left(\frac{1}{2d}-\frac{1}{2d+a}\right)\right] \qquad 5\text{-}1$$

Similarly the potential at (P_2) is

$$V_2 = \frac{I\rho_1}{2\pi}\left[\left(\frac{1}{r}-\frac{1}{r+a}\right)+k\left(\frac{1}{2d-a}-\frac{1}{2d}\right)\right] \qquad 5\text{-}2$$

Hence we have for the potential difference

$$\Delta V = V_1 - V_2$$
$$= \frac{I\rho_1}{2\pi}\left[\frac{2a^2}{r(r^2-a^2)}+k\left(\frac{1}{d}-\frac{1}{2d+a}-\frac{1}{2d-a}\right)\right] \qquad 5\text{-}3$$

The potential drop of A-configuration obtained from field measurement

is, from equation 3-4

$$\Delta V = \frac{I\rho_a}{2\pi}\left[\frac{2a^2}{r(r^2-a^2)}\right] \qquad 3\text{-}4$$

therefore by equating 6-3 and 3-4, and solving for (ρa), the apparent

resistivity becomes

$$\rho_a = \rho_1\left[1 + k\left(\frac{r(r^2-a^2)}{2a^2}\right)\left(\frac{1}{d}-\frac{1}{2d+a}-\frac{1}{2d-a}\right)\right] \qquad 5\text{-}4$$

2.   One Electrode in the Second Medium (Fig. 5-2).

The potential at (P_1) is the same as in case 1. The potential

at (P_2) must be considered as being due to a source of strength

$(1-k)I$ at (C_1) and a sink of $(1-k)(-I) = (k-1)I$ at (C_2).

Direction of Traverse
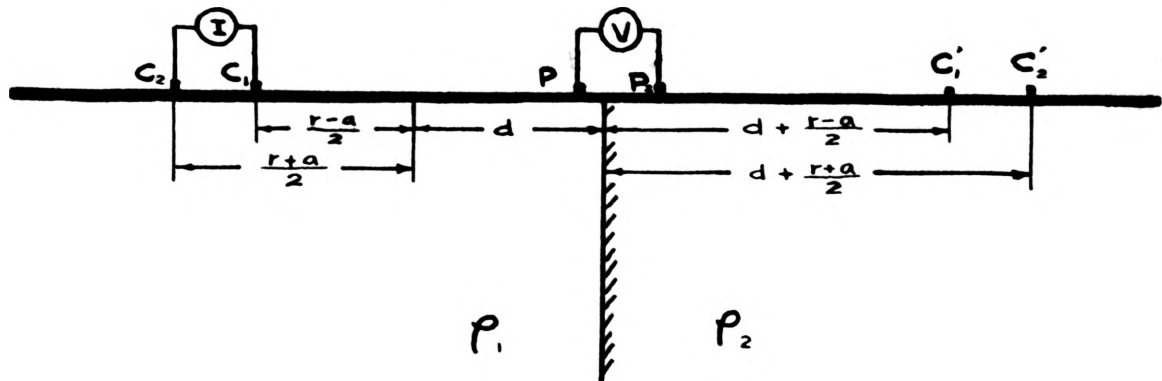
Fig. 5-2 Case 2, A-configuration: One
Electrode In Second Medium

Thus,

$$V_1 = \frac{I\rho_1}{2\pi}\left[\left(\frac{1}{r-a} - \frac{1}{r}\right) + k\left(\frac{1}{2d} - \frac{1}{2d+a}\right)\right]$$ 5-5

$$V_2 = \frac{I\rho_1}{2\pi}\left[(1-k)\left(\frac{1}{r} - \frac{1}{r+a}\right)\right]$$ 5-6

So the total potential difference

$$\Delta V = V_1 - V_2$$

$$= \frac{I\rho_1}{2\pi}\left[\frac{2a^2}{r(r^2-a^2)} + k\left(\frac{1}{2d} - \frac{1}{2d+a} + \frac{1}{r} - \frac{1}{r+a}\right)\right]$$ 5-7

The apparent resistivity can be obtained by combining equations

5-7 and 3-4.

$$\rho_a = \rho_1\left\{1+k\left(\frac{r(r^2-a^2)}{2a^2}\right)\left[\frac{a}{2d(2d+a)} + \frac{a}{r(r+a)}\right]\right\}$$ 5-8

3. Two Electrodes in the Second Medium (Fig. 5-3).

In this case, potentials at (P_1) and (P_2) are both considered as due to a source of strength $(1-k)I$ at (C_1) and $(k-1)I$ at (C_2).
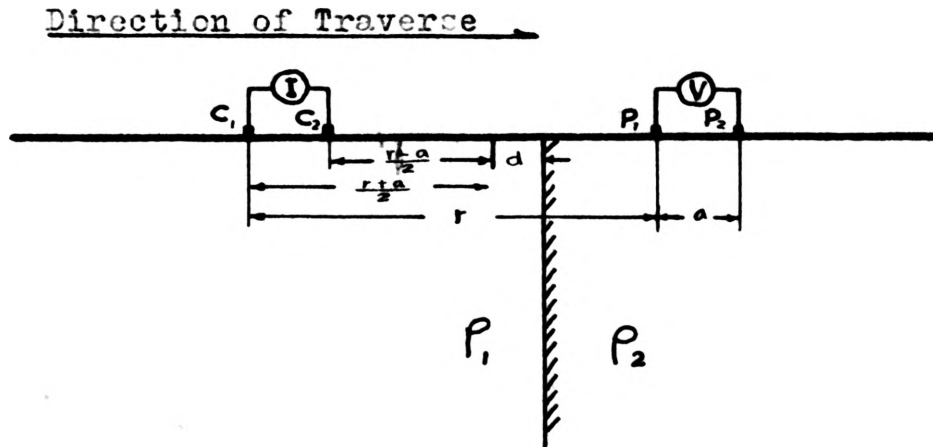
Fig. 5-3 Case 3, A-configuration: Two Electrodes In Second Medium

$$V_1 = \frac{I\rho}{2\pi}\left[(1-k)(\frac{1}{r-a} - \frac{1}{r})\right] \qquad \text{5-9}$$

$$V_2 = \frac{I\rho}{2\pi}\left[(1-k)(\frac{1}{r} - \frac{1}{r+a})\right] \qquad \text{5-10}$$

So, for the total potential difference

$$\Delta V = V_1 - V_2$$
$$= \frac{I\rho}{2\pi}(1-k)\left[\frac{2a^2}{r(r^2-a^2)}\right] \qquad \text{5-11}$$

Therefore the apparent resistivity becomes

$$\rho_a = (1-k)\,\rho_1 \qquad \text{5-12}$$

4. Three Electrodes in the Second Medium Fig. 5-4).

In this case the potentials at (P_1) and (P_2) are attributed

to (I) at (C_1), (k-1)I at (C_2), and (-kI) at the image (C_1')
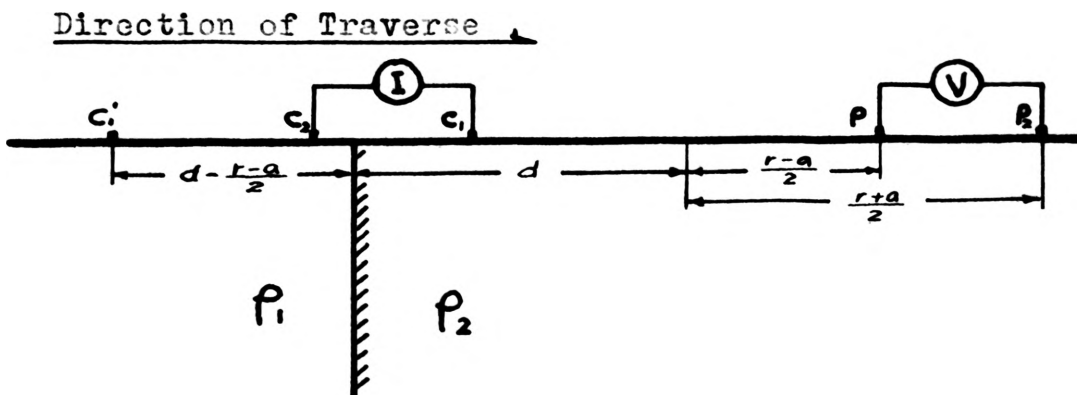
Fig. 5-4 Case 4, A-configuration: Three
Elect odes In Second Medium

$$V_1 = \frac{I}{2\pi}\left[\rho_2(\frac{1}{r-a} + \frac{k}{2d}) + \frac{\rho_1(k-1)}{r}\right] \qquad 5\text{-}13$$

$$V_2 = \frac{I}{2\pi}\left[\rho_2(\frac{1}{r} + \frac{k}{2d+a}) + \frac{\rho_1(k-1)}{2d+a}\right] \qquad 5\text{-}14$$

So the **total potential difference**

$$\Delta V = V_1 - V_2$$

$$= \frac{I}{2\pi}\left\{\rho_2\left[\frac{a}{r(r-a)} + k(\frac{a}{2d(2d+a)})\right] + \rho_1(k-1)(\frac{1}{r} - \frac{1}{2d+a})\right\} \qquad 5\text{-}15$$

Therefore the **apparent resistivity** becomes

$$\rho_a = \frac{r(r^2-a^2)}{2a^2}\left\{\rho_2\left[\frac{a}{r(r-a)} + k\frac{a}{2d(2d+a)}\right] + \rho_1(k-1)(\frac{1}{r} - \frac{1}{2d+a})\right\} \; 5\text{-}16$$

5. Four Electrodes in the Second Medium (Fig. 5-5).

The potential equations in this case are similar to Case 1.

According to equation 2-8, the reflection factor in the medium (ρ_2) is k_{21}, where

$$k_{21} = \frac{\rho_1 - \rho_2}{\rho_1 + \rho_2} = -k_{12}$$
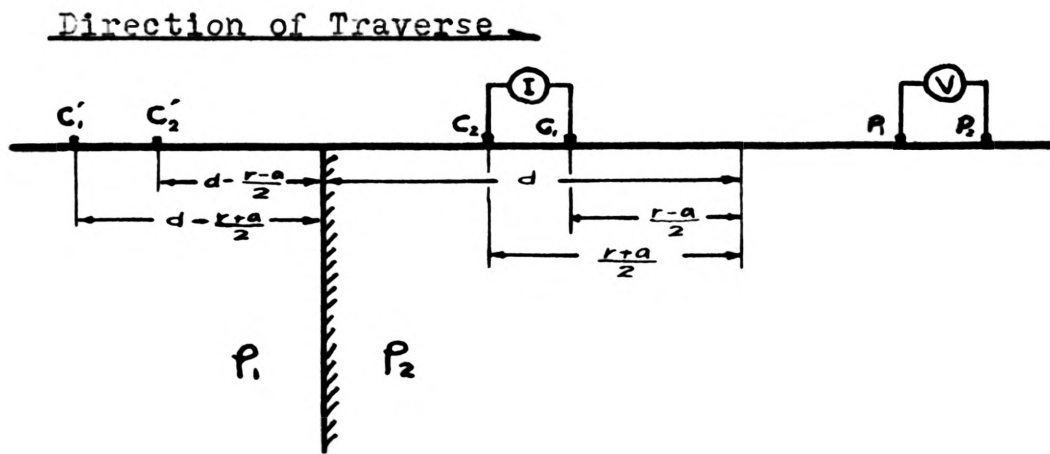
Fig. 5-5 Case 5, A-configuration: All
Electrodes In Second Medium

The potentials will be considered as due to a source (I) at (C_1), a sink $-I$ at (C_2), and images $(-k)I$ at (C_1'), $(-k)(-I) = kI$ at (C_2'). Thus

$$V_1 = \frac{I\rho_2}{2\pi}\left[\left(\frac{1}{r-a} - \frac{1}{r}\right) + k\left(\frac{1}{2d-a} - \frac{1}{2d}\right)\right] \qquad 5\text{-}17$$

$$V_2 = \frac{I\rho_2}{2\pi}\left[\frac{1}{r} - \frac{1}{r+a} + k\left(\frac{1}{2d} - \frac{1}{2d+a}\right)\right] \qquad 5\text{-}18$$

The potential difference is

$$\Delta V = V_1 - V_2$$

$$= \frac{I\rho_2}{2\pi}\left[\frac{2a^2}{r(r^2-a^2)} + k\left\{\frac{a}{2d(2d-a)} - \frac{a}{2d(2d+a)}\right\}\right]$$

$$= \frac{I\rho_2}{2\pi}\left[\frac{2a^2}{r(r^2-a^2)} + k\left(\frac{a^2}{d(4d^2-a^2)}\right)\right] \qquad 5\text{-}19$$

The apparent resistivity becomes

$$\rho_a = \rho_2 \left[1 + k \; \left(\frac{r(r^2 - a^2)}{2d(4d^2 - a^2)} \right) \right]$$

C.. Solutions for B-Configuration.

    1. Four Electrodes in the First Medium (Fig. 5-6).

    As shown in Case 1 of A-configuration, (d) is the distance from the center of the electrode system to the plane of discontinuity. Assume a current source of (I) at (C_1) and a sink $(-I)$ at (C_2). The potential at the electrodes (P_1) and (P_2) will depend on the strength of (I) and $(-I)$ which is introduced into the earth by a generator, and their images at (C_1') and (C_2') which is the result of reflection from the fault plane. The potential at (P_1) due to the source (I) at (C_1) is $(I\rho_1/2\pi)(\frac{1}{a})$, due to sink $(-I)$ at (C_2) is $\frac{-I\rho_1}{2\pi}(\frac{1}{r})$. The potential resulting from the image at (C_1) is $\frac{kI}{2}(\frac{1}{2d+r})$, and that due to the image at (C_2') is $\frac{-kI\rho_1}{2\pi}(\frac{1}{2d-a})$.

Direction of Traverse
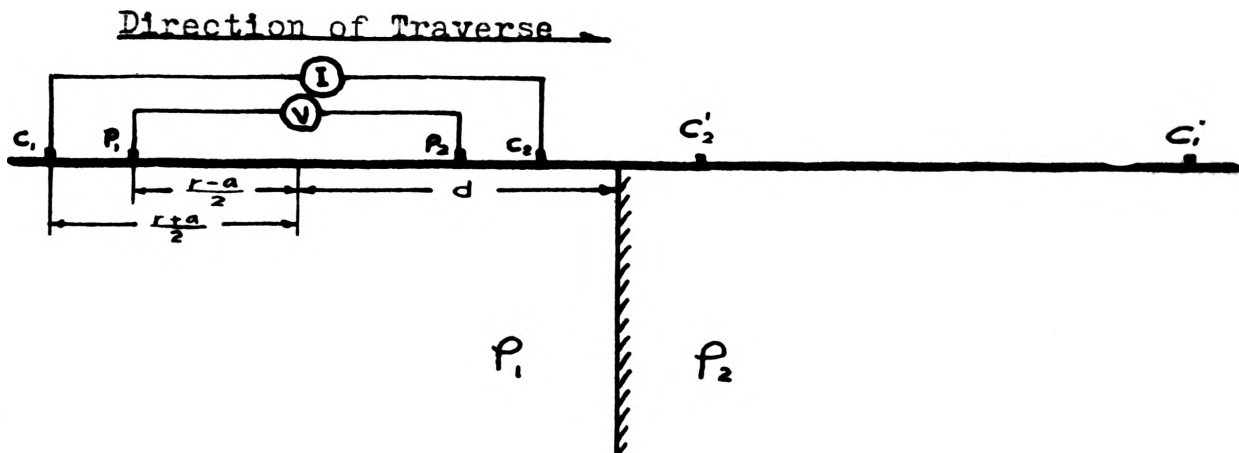
Fig. 5-6 Case 1, B-configuration:
Four Electrodes In The First Medium

Therefore the total potential at (P_1) is

$$V_1 = \frac{I\rho_1}{2\pi}\left[\left(\frac{1}{a} - \frac{1}{r}\right) + k\left(\frac{1}{2d+r} - \frac{1}{2d-a}\right)\right] \qquad 5\text{-}21$$

Similarly the potential at (P_2) is

$$V_2 = \frac{I\rho_1}{2\pi}\left[\left(\frac{1}{r} - \frac{1}{a}\right) + k\left(\frac{1}{2d+a} - \frac{1}{2d-r}\right)\right] \qquad 5\text{-}22$$

Hence the potential difference is

$$\triangle V = V_1 - V_2$$

$$= \frac{I\rho_1}{2\pi}\left[\frac{2(r-a)}{ar} + 4kd\left(\frac{1}{4d^2-r^2} - \frac{1}{4d^2-a^2}\right)\right] \qquad 5\text{-}23$$

Combining equations 3-7 and 5-24, solve for the apparent resistivity (ρ_a).

$$\rho_a = \rho_1\left[1 + 4k\left(\frac{ard}{2(r-a)}\right)\left(\frac{1}{4d^2-r^2} - \frac{1}{4d^2-a^2}\right)\right] \qquad 5\text{-}24$$

2.   One Electrode in the Second Medium (Fig. 5-7).

The potential difference $V_1 - V_2$ due to the source (I) at (C_1) and its image (C_1') will be the same as in Case 1. However, the potential due to (C_2) in the second medium (ρ_2) is considered as being due to a source of strength $(1-k)(-I) = (k-1)I$. The potential at (P_1) is therefore the sum of the potentials due to a source (I) at (C_1), an image (kI) at (C_1'), and a source $(k-1)$ at (C_2).
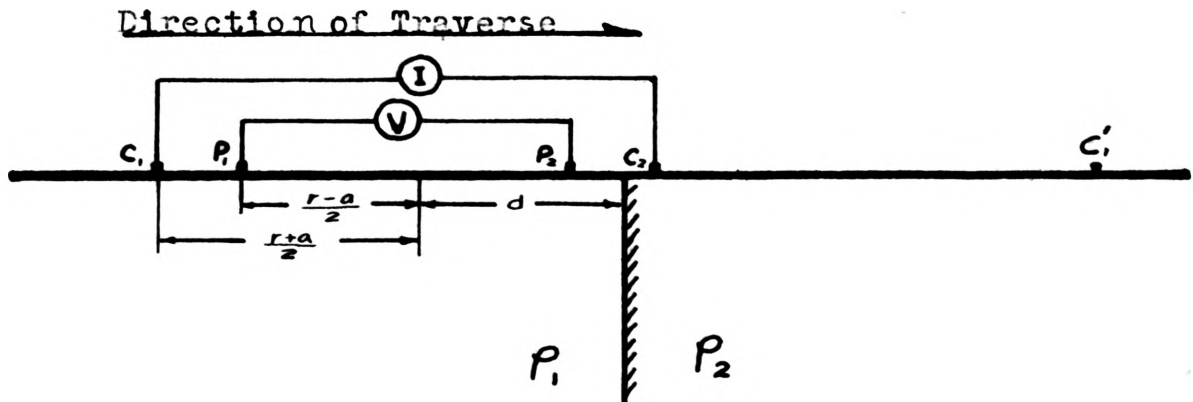
Fig. 5-7   Case 2, B-configuration: One
Electrode In The Second Medium

Thus

$$V_1 = \frac{I}{2\pi}\left[\rho_1(\frac{1}{a} - \frac{k}{2d+r}) + \frac{\rho_2(k-1)}{r}\right]$$

5-25

The potential at (P_2) is similarly

$$V_2 = \frac{I}{2\pi}\left[\rho_1(\frac{1}{r} + \frac{k}{2d+a}) + \frac{\rho_2(k-1)}{a}\right]$$

5-26

Therefore

$$\Delta V = V_1 - V_2$$

$$\frac{I}{2\pi}\left\{\rho_1\left[(\frac{r-a}{ar}) + k\frac{(r-a)}{(2d+a)(2d+r)}\right] + \rho_2\left[\frac{(k-1)(a-r)}{ar}\right]\right\}$$

5-27

From equation 3-7, for the actual field result

$$\Delta V = \frac{I\rho_a}{2\pi}\left[\frac{2(r-a)}{ar}\right]$$

Therefore by equating equations 5-27 and 3-7,

$$\rho_a = \rho_1\left[\frac{1}{2} + k\left(\frac{ar}{(2d+r)(2d+a)}\right)\right] + \rho_2(\frac{1-k}{2})$$

5-28

3. Two Electrodes in Each Medium (Fig. 5-8)
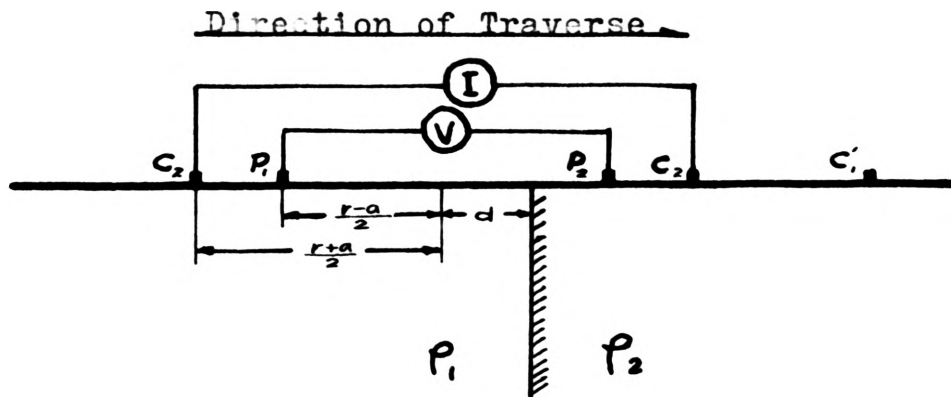
Fig. 5-3 Case 3, B-configuration: Two Electrodes In Each Medium

The potential at (P_1) is due to the source (I) at (C_1), (kI) at (C_1'), and $(k-1)$ at (C_2).

$$V_1 = \frac{I}{2\pi}\left[\rho_1(\frac{1}{a} + \frac{k}{2d+r}) + \frac{\rho_2(k-1)}{r}\right] \qquad 5\text{-}29$$

The potential at (P_2) is considered as due to $(1-k)I$ at (C_1), $(-I)$ at (C_2), and $(-k)(-I) = kI$ at (C_2'). So that

$$V_2 = \frac{I}{2\pi}\left[\rho_2(\frac{k}{r+2d} - \frac{1}{a}) + \rho_1\frac{(1-k)}{r}\right] \qquad 5\text{-}30$$

Thus the potential difference

$$\Delta V = V_1 - V_2$$
$$= \frac{I}{2\pi}\left\{\rho_1\left[\frac{r-a}{ar} + k\,(\frac{2(d+r)}{r(2d+r)}\right] + \rho_2\left[\frac{r-a}{ar} + k\,(\frac{2d}{r(r+2d)})\right]\right\} \qquad 5\text{-}31$$

Therefore the apparent resistivity becomes

$$\rho_a = \rho_1\left[\frac{1}{2} + k\,(\frac{a(d+r)}{(r-a)(2d+r)})\right] + \rho_2\left[\frac{1}{2} + k(\frac{da}{(r-a)(r+2d)})\right] \qquad 5\text{-}32$$

Note that in this case the value of (d) is decreasing when the center of the configuration approaches the fault plane. After the center point has passed through the fault plane, the distance (d) is considered negative. This is the only case in which we shall consider the sign of the distance (d). For simplicity, (d) is considered positive in all other cases.

4.   Three Electrodes in the Second Medium (Fig. 5-9).
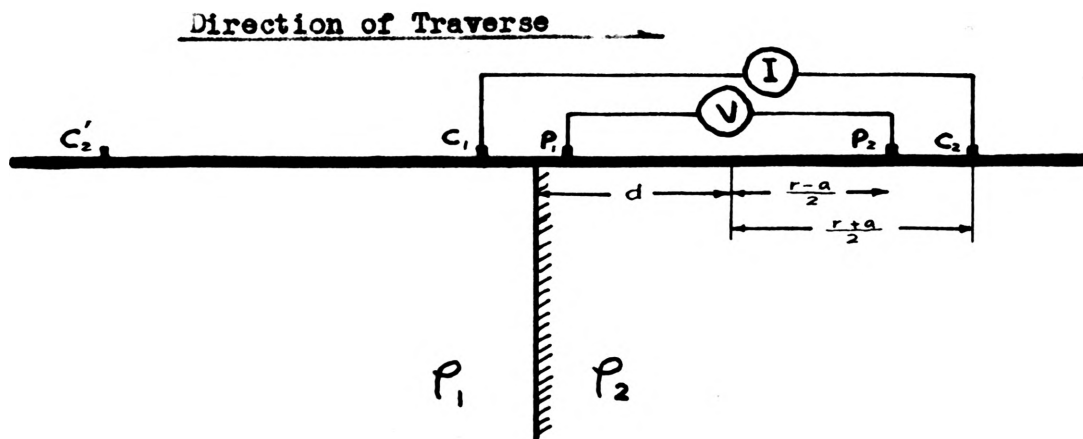
Fig. 5-9 Case 4, B-configuration: Three Electrodes In Second Medium

In this case the potentials at (P_1) and (P_2) are due to the sources $(1-k)I$ at (C_1), $(-I)$ at (C_2), and kI at the image (C_2').

$$V_1 = \frac{I}{2\pi}\left[\frac{\rho_1(1-k)}{a} + \rho_2\left\{\frac{k}{2d+a} - \frac{1}{r}\right\}\right] \qquad 5\text{-}33$$

$$V_2 = \frac{I}{2\pi}\left[\frac{\rho_1(1-k)}{r} + \rho_2\left\{\frac{k}{2d+r} - \frac{1}{a}\right\}\right] \qquad 5\text{-}34$$

The potential difference is

$$\Delta V = \frac{I}{2\pi}\left\{\rho_1\left[\frac{(1-k)(r-a)}{ar}\right] + \rho_2\left[\frac{k(r-a)}{(2d+a)(2d+r)} + \frac{r-a}{ar}\right]\right\} \qquad 5\text{-}35$$

Therefore

$$\rho_a = \rho_1\left[\frac{1-k}{2}\right] + \rho_2\left[1 + k\left(\frac{ar}{(2d+a)(2d+r)}\right)\right] \qquad 5\text{-}36$$

5. All Electrodes in the Second Medium (Fig. 5-10).
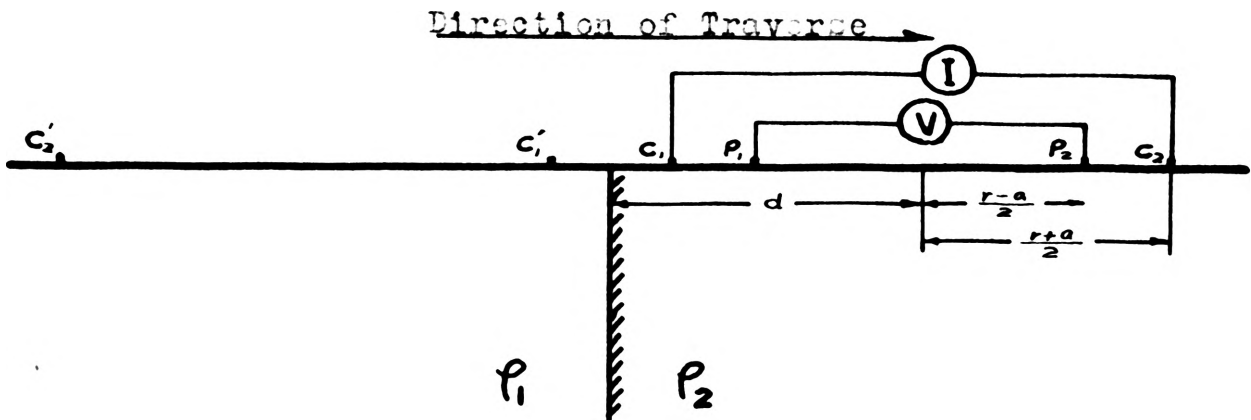
Fig. 5-10 Case 5, B-configuration: All
Electrodes In Second Medium

This case is similar to Case 1 except the reflection factor is $(-k)$.

$$V_1 = \frac{I\rho_2}{2\pi}\left[\left(\frac{1}{a} - \frac{1}{r}\right) + k\left(\frac{1}{2d-r} - \frac{1}{2d+a}\right)\right] \qquad 5\text{-}37$$

$$V_2 = \frac{I\rho_2}{2\pi}\left[\left(\frac{1}{r} - \frac{1}{a}\right) + k\left(\frac{1}{2d-a} - \frac{1}{2d+r}\right)\right] \qquad 5\text{-}38$$

The potential difference is

$$\Delta V = \frac{I\rho_2}{2\pi}\left[\frac{2(r-a)}{ar} + k\left(\frac{4d}{4d^2-r^2} - \frac{4d}{4d^2-a^2}\right)\right]$$

$$= \frac{I\rho_2}{2\pi}\left[\frac{2(r-a)}{ar} + 4kd\left(\frac{1}{4d^2-r^2} - \frac{1}{4d^2-a^2}\right)\right] \qquad 5\text{-}39$$

Therefore the apparent resistivity is

$$\rho_a = \rho_2\left\{1 + 4k\left[\frac{ard}{2(r-a)}\right]\left[\frac{1}{4d^2-r^2} - \frac{1}{4d^2-a^2}\right]\right\} \qquad 5\text{-}40$$

VI. NEW CONFIGURATIONS APPLIED TO DEPTH PROBES
IN TWO LAYERED MEDIA

One of the most important interpretations of earth resistivity data is that for a two layered media problem. The potential distribution in a two layered earth problem has been investigated by many workers. The earth is assumed to consist of two horizontal layers of different conductivity. Early investigation had dealt with the potential distribution about a point electrode placed on the earth's surface. As long ago as 1873, J. C. Maxwell treated the problem by calculating a system of electrode images. In 1929, Hummel applied the method of images to the problem of an earth underlying a single horizontal parallel overburden, but gave the results without showing their derivation. The form of the derivation was indicated and some numerical values were given. He introduced the concept of apparent resistivity based on Wenner's formulation (1915), which had been presented earlier. This was followed by several papers (TAGG, 1930; ROMAN, 1931; HUBBERT, 1934), repeating, extending the results, or furnishing tables of resistivity values for various electrode spacings, reflection factors, and overburden thicknesses. The method of images is direct and relatively simple. It leads to an infinite series whose evaluation may prove tedious, but which requires little advanced mathematics.

Hummel's technique is based on the premise that there is an infinite number of current sources at the positions of mirror images of the electrodes as they would be reflected optically by the parallel

interfaces of discontinuity. Because each reflection involves a loss
of intensity (as in the analogous optical case) and successive
reflections correspond to increasingly distant sources, it is only
necessary to consider the effect of the first few reflections to
obtain a useful approximation of the potential. In the case of a
surface layer of resistivity ρ_1 overlying an infinitely thick parallel
substratum of resistivity ρ_2, the apparent resistivity ρ_a is, for the
Wenner configuration,

$$\rho_a = \rho_1 \left\{ 1 + 4 \sum_{n=1}^{\infty} k^n \left[\frac{1}{(1 + (\frac{2nh}{a})^2)^{\frac{1}{2}}} - \frac{1}{(4 + (\frac{2nh}{a})^2)^{\frac{1}{2}}} \right] \right\} \qquad 6\text{-}1$$

where (a) is the electrode separation for the Wenner arrangement,
(h) is the thickness of the ρ_1 layer, and (k), the resistivity contrast,
is given by equation 2-8. Equation 6-1 is an infinite series with
the n-th term having the form

$$k^n \left[\frac{1}{(1+(\frac{2nh}{a})^2)^{\frac{1}{2}}} - \frac{1}{(4+\frac{2nh}{a})^2)^{\frac{1}{2}}} \right] \qquad 6\text{-}2$$

Since (k) is always less than unity, the series converges, i.e.,
the terms approach zero as (n) increases, and only a limited number
of terms (each corresponding to a successive "multiple reflection")
is needed to reduce the error to less than some chosen limit.

In 1930, Tagg presented a method of interpretation of resistivity
data obtained with the Wenner configuration. Detailed discussions
of theoretical considerations, derivations of formulas, and a method
of interpretation similar to Tagg's method have been published by
Irwin Roman (1931, 1933, 1941, 1953, 1959, 1960). For calculations
involving formulas 6-1 and 6-2, it is very convenient to use the
tables given by Roman, 1931.

Similar formulas described above may be obtained for both the A-configuration and the B-configuration by applying the same method of images. Consider the two layer problem of a homogeneous and isotropic medium of resistivity ρ_1 and uniform thickness (h) overlying a semi-infinite medium of finite resistivity ρ_2. The depth to the interface is to be investigated using an expanding electrode probe for which the electrode pair separation (r) is expanded but the electrode spacing (a) is kept constant. See Fig. 6-1.
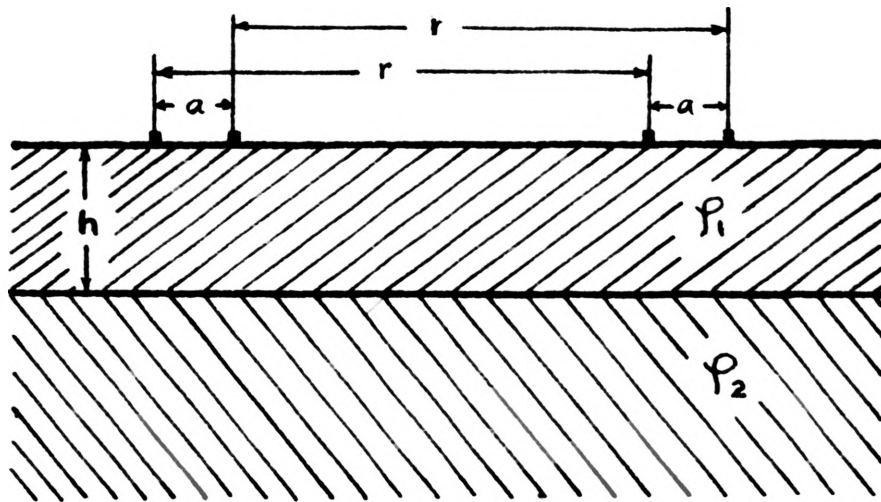
Fig. 6-1 Two Layer Case

A. General Theory.

In Fig. 6-2, the upper layer is bounded by air (resistivity $\rho_0 = \infty$). If the current is supplied at two points, (C_1) and (C_2), the potential distribution at the surface can be calculated by considering a source (I) at (C_1), a sink (-I) at (C_2), and the images of this source and sink that are produced by reflections on the resistive formation of

lower boundary and on the earth s surface. The source (I) is
reflected at the ρ_1-ρ_2 boundary and produces the image I_1 = (kI).
The value of (k) is equal to $(\rho_2-\rho_1)/(\rho_2+\rho_1)$, for it applies to the
formation boundary of ρ_1 and ρ_2. The image I_1 is now reflected at
the earth s surface and produces the image I_2 = k kI above.. In this
case (k) is applied to the boundary between the upper medium and air.
Because the resistivity of the air (ρ_o) is infinite, (k) is one
(Equation 2-9). Hence, the image I_1' = kI. The image source I_1', will
be reflected similarly as I_1. The potential at any surface point
will therefore result from a summation of an infinite series of
images. Thus, I_1 = kI at depth 2h; I_1' = kI at a height 2h; I_2 = $k^2 I$
at a depth 4h; I_2' = $k^2 I$ at a height 4h, and I_n = $k^n I$ at a depth at
2nh and I_n' = $k^n I$ at a height 2nh. Because I_n = I_n', $I_n + I_n'$ = $2k^n I$,
and the potential at any point on the surface is given by the
equation

$$V = \frac{\rho_1}{2\pi}\left[\frac{I}{r} + \sum_{n=1}^{\infty} \frac{2k^n I}{r_n}\right] \qquad\qquad 6\text{-}3$$

where (r_n) is the distance from the n-th image to the potential
electrode.

By applying equation 6-3, we can find the potential at each
potential electrode. By applying equations 1-1, 1-2 and 1-3, we
can obtain theoretical resistivity values for the A-configuration
and the B-configuration.
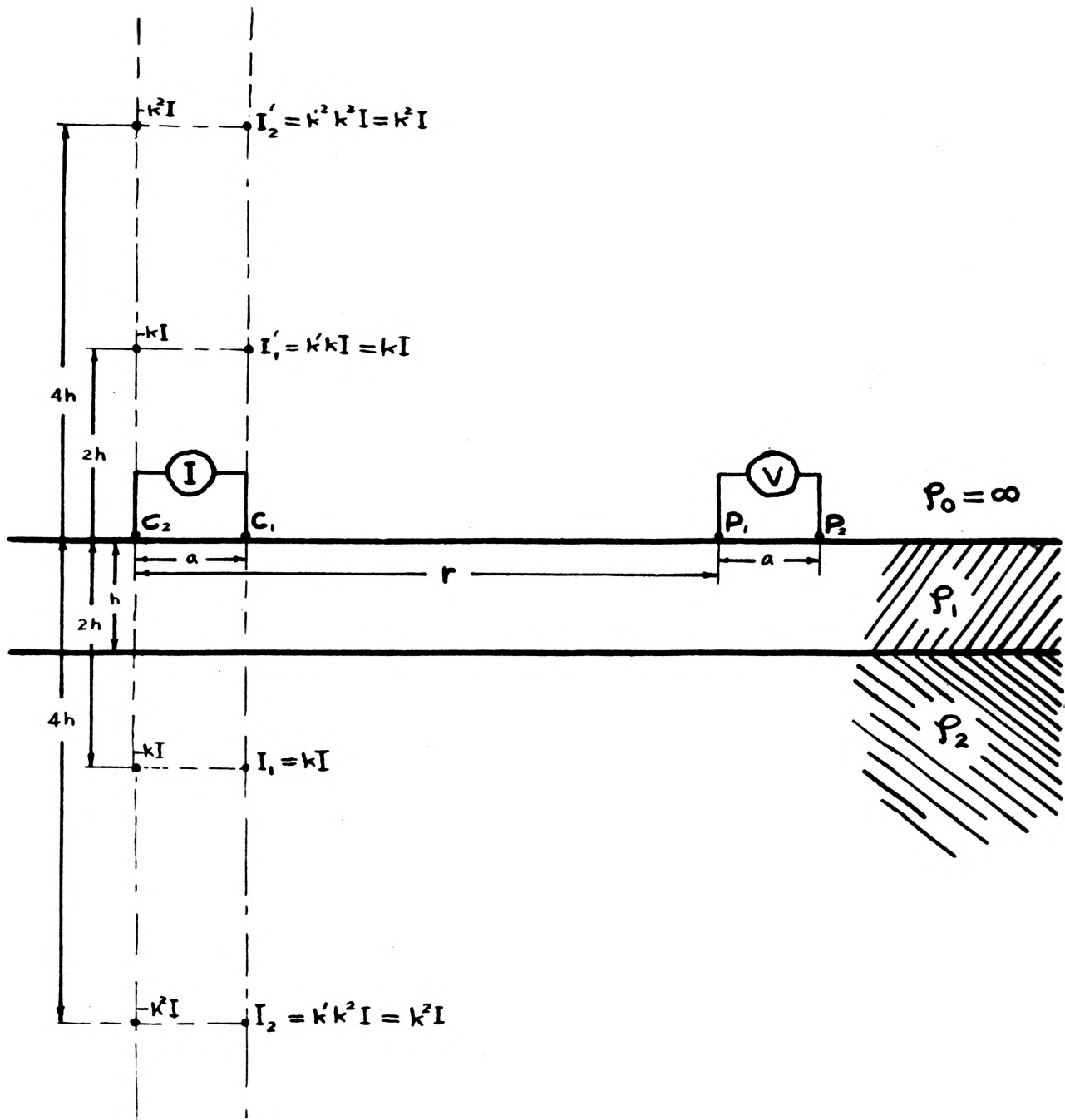
Fig. 6-2   Two Layer Case
A-configuration

B.   **Solutions for the A-Configuration.**

Referring to Fig. 6-2 and by applying equation 6-3, we obtain

$$V_1 = \frac{I\rho}{2\pi}\left\{\frac{1}{r-a} - \frac{1}{r} + \sum_{n=1}^{\infty}2k^n\left[\frac{1}{[(r-a)^2+4n^2h^2]^{\frac{1}{2}}} - \frac{1}{[r^2+4n^2h^2]^{\frac{1}{2}}}\right]\right\} \qquad 6\text{-}4$$

$$V_2 = \frac{I\rho}{2\pi}\left\{\frac{1}{r} - \frac{1}{r-a} + \sum_{n=1}^{\infty}2k^n\left[\frac{1}{[r^2+4n^2h^2]^{\frac{1}{2}}} - \frac{1}{[(r+a)^2+4n^2h^2]^{\frac{1}{2}}}\right]\right\} \qquad 6\text{-}5$$

therefore

$$\Delta V = \frac{I\rho}{2\pi}\left\{\frac{2a^2}{r(r^2-a^2)} + \sum_{n=1}^{\infty}2k^n\left[\frac{1}{[(r-a)^2+4n^2h^2]^{\frac{1}{2}}}\right.\right.$$
$$\left.\left. + \frac{1}{[(r+a)^2+4n^2h^2]^{\frac{1}{2}}} - \frac{2}{[r^2+4n^2h^2]^{\frac{1}{2}}}\right]\right\} \qquad 6\text{-}6$$

In field operation, the apparent resistivity value is obtained from the reading of current (I) and potential difference ΔV. Thus, equations 3-3 and 3-4

$$\Delta V = \frac{I\rho_a}{2\pi}\left[\frac{2a^2}{r(r^2-a^2)}\right]$$

or

$$\rho_a = 2\pi\frac{\Delta V}{I}\left[\frac{r(r^2-a^2)}{2a^2}\right]$$

with equation 6-6 to obtain

$$\rho_a\left[\frac{2a^2}{r(r^2-a^2)}\right] = \rho_1\left\{\frac{2a^2}{r(r^2-a^2)} + \sum_{n=1}^{\infty}2kn\left[\frac{1}{[(r-a)^2+4n^2h^2]^{\frac{1}{2}}}\right.\right.$$
$$\left.\left. + \frac{1}{[(r+a)^2+4n^2h^2]^{\frac{1}{2}}} - \frac{2}{[r^2+4n^2h^2]^{\frac{1}{2}}}\right]\right\} \qquad 6\text{-}7$$

or

$$\rho_a = \rho_1\left\{1 + \left[\frac{r(r^2-a^2)}{2a^2}\right]\sum_{n=1}^{\infty}2k^n\left[\frac{1}{[(r-a)^2+4n^2h^2]^{\frac{1}{2}}}\right.\right.$$
$$\left.\left. + \frac{1}{[(r+a)^2+4n^2h^2]^{\frac{1}{2}}} - \frac{2}{[r^2+4n^2h^2]^{\frac{1}{2}}}\right]\right\} \qquad 6\text{-}7a$$

If the constant electrode spacing (a) is taken as unit distance, the electrode pair separation (r) can be expressed in terms of (a). When r = xa,

$$\rho_a = \rho_i\left(1 + x(x^2-1)\sum_{n=1}^{\infty} 2k^n\left\{\frac{1}{[(x-1)^2 + 4n^2\frac{h^2}{a^2}]^{\frac{1}{2}}}\right.\right.$$

$$\left.\left. + \frac{1}{[(x+1)^2 + 4n^2\frac{h^2}{a^2}]^{\frac{1}{2}}} - \frac{2}{[x^2 + 4n^2\frac{h^2}{a^2}]^{\frac{1}{2}}}\right\}\right) \qquad 6\text{-}7b$$

In this configuration, if (r) increases, that is, (x) increases, the terms of the summation will become smaller. This can be found from equation 6-7b. As r = xa increases, the values $(x-1)^2$, $(x+1)^2$ and X^2 in the function will become nearly the same, so the total value in the summation approaches zero. However, the multiplying factor before the summation is $x(x^2-1)$, which increases rapidly as r = xa increases. This will more than compensate for the decrease inside the summation. The terms in the summation can be considered as the effect of potential values due to reflected images. When (r) is large, this effect will be larger than the corresponding effect for the Wenner configuration.

C.   Solutions for the B-Configuration.

Referring to Fig. 6-3, and equation 6-3, the potential at each potential electrode of the B-configuration can be calculated. The distance from each image at depth (2nh) or height (2nh) to electrodes P_1 and P_2 are $[a^2 + (2nh)^2]^{\frac{1}{2}}$ and $[r^2 + (2nh)^2]^{\frac{1}{2}}$.   (see Fig. 6-3).
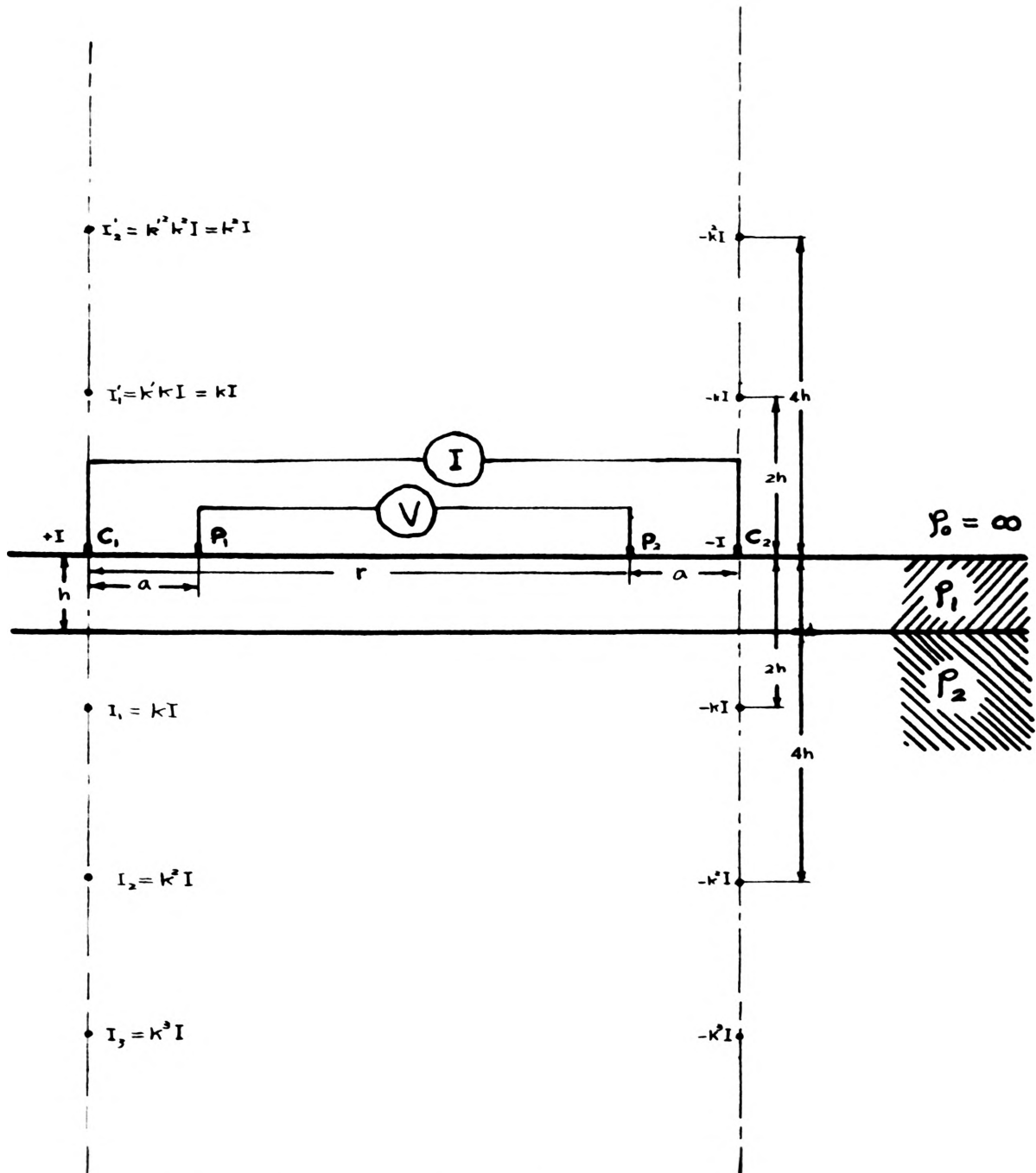
Fig. 6-3 Two Layer Case
B-configuration

Therefore

$$V_1 = \frac{I\rho_1}{2\pi}\left(\frac{1}{a} - \frac{1}{r} + \sum_{n=1}^{\infty} 2k^n \left\{ \frac{1}{[a^2+(2nh)^2]^{\frac{1}{2}}} - \frac{1}{[r^2+(2nh)^2]^{\frac{1}{2}}} \right\} \right) \qquad 6\text{--}8$$

$$V_2 = \frac{I\rho_1}{2\pi}\left(\frac{1}{r} - \frac{1}{a} + \sum_{n=1}^{\infty} 2k^n \left\{ \frac{1}{[r^2+(2nh)^2]^{\frac{1}{2}}} - \frac{1}{[a^2+(2nh)^2]^{\frac{1}{2}}} \right\} \right)$$

$$\Delta V = \frac{I\rho_1}{2\pi}\left(\frac{2(r-a)}{ar} + 4\sum_{n=1}^{\infty} k^n \left\{ \frac{1}{[a^2+(2nh)^2]^{\frac{1}{2}}} - \frac{1}{[r^2+(2nh)^2]^{\frac{1}{2}}} \right\} \right) \qquad 6\text{--}9$$

Equating 3-7 and 6-9 the apparent resistivity in the B-configuration is

$$\rho_a \left[\frac{2(r-a)}{ar}\right] = \rho_1 \left(\frac{2(r-a)}{ar} + 4\sum_{n=1}^{\infty} k^n \left\{ \frac{1}{[a^2+(2nh)^2]^{\frac{1}{2}}} - \frac{1}{[r^2+(2nh)^2]^{\frac{1}{2}}} \right\} \right) \quad 6\text{--}10$$

If we let $r = xa$, we obtain

$$\rho_a = \rho_1 \left(1 + \frac{2x}{(x-1)} \sum_{n=1}^{\infty} k^n \left\{ \frac{1}{[1+(\frac{2nh}{a})^2]^{\frac{1}{2}}} - \frac{1}{[x^2+(\frac{2nh}{a})^2]^{\frac{1}{2}}} \right\} \right) \qquad 6\text{--}10a$$

In this theoretical two layer case, if the distance (r) become much larger than (a), for the first few terms of the summation the difference of the two terms inside the summation will become larger because the second term becomes very small. Therefore the depth of penetration to the subsurface structure will increase with an increase of distance (r).

The multiplying value in front of the summation is $2x/(x-1)$. The apparent resistivity obtained over a two layered media by use of the Wenner configuration is

$$\rho_a = \rho_1 \left(1 + 4\sum_{n=1}^{\infty} k^n \left\{ \frac{1}{[1+(\frac{2nh}{a})^2]^{\frac{1}{2}}} - \frac{1}{[4+(\frac{2nh}{a})^2]^{\frac{1}{2}}} \right\} \right)$$

Comparing this equation with equation 6-10a, it is easy to see that when x = 2, equation 6-10a is the same as the Wenner configuration. As the value of (x) increases, the multiplying value before the

summation sign will decrease. Therefore the total resistivity value obtained from the B-configuration is smaller than that from the Wenner configuration. However, the second term inside the summation will decrease rapidly. As (x) becomes larger, this multiplying value will approach 2. The second term inside the summation will become very small. Therefore the B-configuration has less than 1 but more than 1/2 times the resolving power of the Wenner configuration. The advantage of the facility of continuous operation may compensate for this decreased resolving power.

VII. MODEL EXPERIMENTS FOR NEW CONFIGURATION

Theoretical analyses and apparent resistivities for the new con-
figurations, for several assumed simple geologic conditions, have been
presented in preceeding chapters. To test these analyses, model
investigations were made by applying the A-configuration and the B-con-
figuration to a model tank of size three by six feet and twenty
inches deep. This tank was formerly built by A. H. Kwentus (1960)
for the purpose of resistivity model investigations. The instrument
used in the measurements is a Megger Ground Tester (see LEE, 1928;
LOW, et. al., 1932). The tank was filled with brine water having a
resistivity of 180 ohm-cms. Theoretical curves calculated from
equations obtained from chapters V and VI were plotted with each
equivalent experimental curve.

A. Instrumental Limits and Wall Effect.

Measurements were first taken over the brine water with no model
present in order to determine the characteristics of each configuration
and the effects of the wall and bottom of the tank. The fixed
electrode spacing (a) was set at one inch and the electrode pair
separation (r) was expanded in units of (a). The results are given
in Tables 7-1 and 7-2. The results are also plotted as resistivity
curves in Figure 7-1 and 7-2.

The Megger Ground Tester has four resistance ranges, 0-1000 ohms,
0-100 ohms, 0-10 ohms and 0-1 ohms. The meter can be read accurately

Table 7-1

A-Configuration Depth Probe
Over a Homogeneous Brine Water

Electrode Pair Separation (r) Inches	Configuration Factor (F) Inches	Configuration Resistance (R) Measured (ohm)	Resistivity (P_i) (ohm-cms)
2	3	3.77	180.04
3	12	0.957	183
4	30	0.370	177
5	60	0.174	166.7
6	105	0.093	159
7	168	0.053	147.4
8	252	0.032	128.4
9	360	0.019	109.2
10	495	0.010	79.1

Table 7-2

B-Configuration Depth Probe Over
a Homogeneous Brine Water

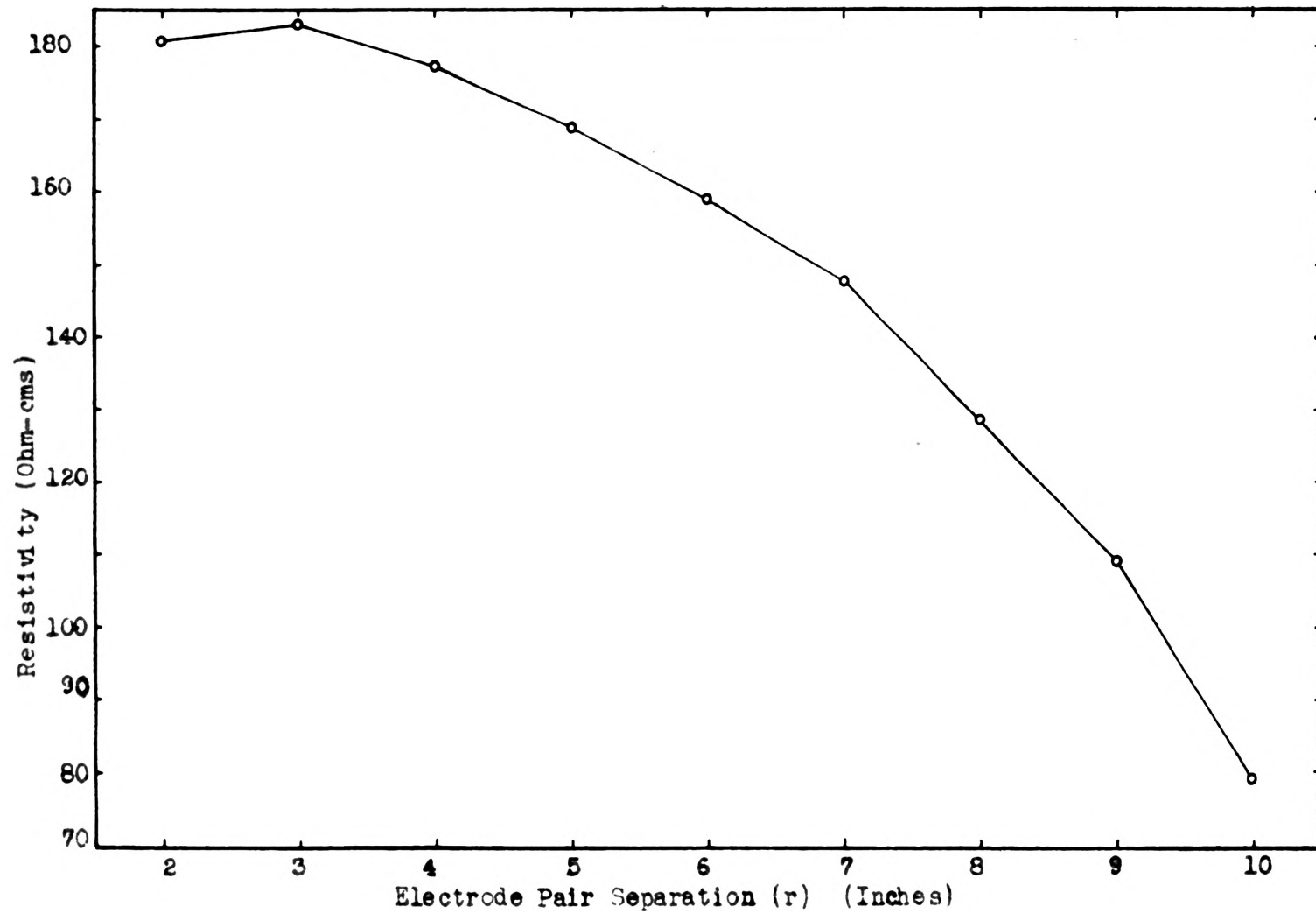| Electrode Pair Separation (r)	Configuration Factor (F)	Configuration Resistance (R)	Resistivity (ρ)
Inches	Inches	(Ohms)	(Ohm-cms)
2	1	11.4	182
3	0.75	15.1	181
4	0.66	17.2	181.3
5	0.625	18.3	182.4
6	0.600	19.1	182.8
7	0.583	19.9	185
8	0.571	20.3	185
9	0.562	20.6	185.6
10	0.556	20.9	185.4
11	0.550	21.2	186
12	0.546	21.4	186.2
13	0.542	21.6	187
14	0.538	21.8	187.3
15	0.536	21.9	187.5
16	0.533	22.1	188
17	0.531	22.2	188.2
18	0.5294	22.3	188.3
19	0.528	22.5	188.6
20	0.526	22.6	190

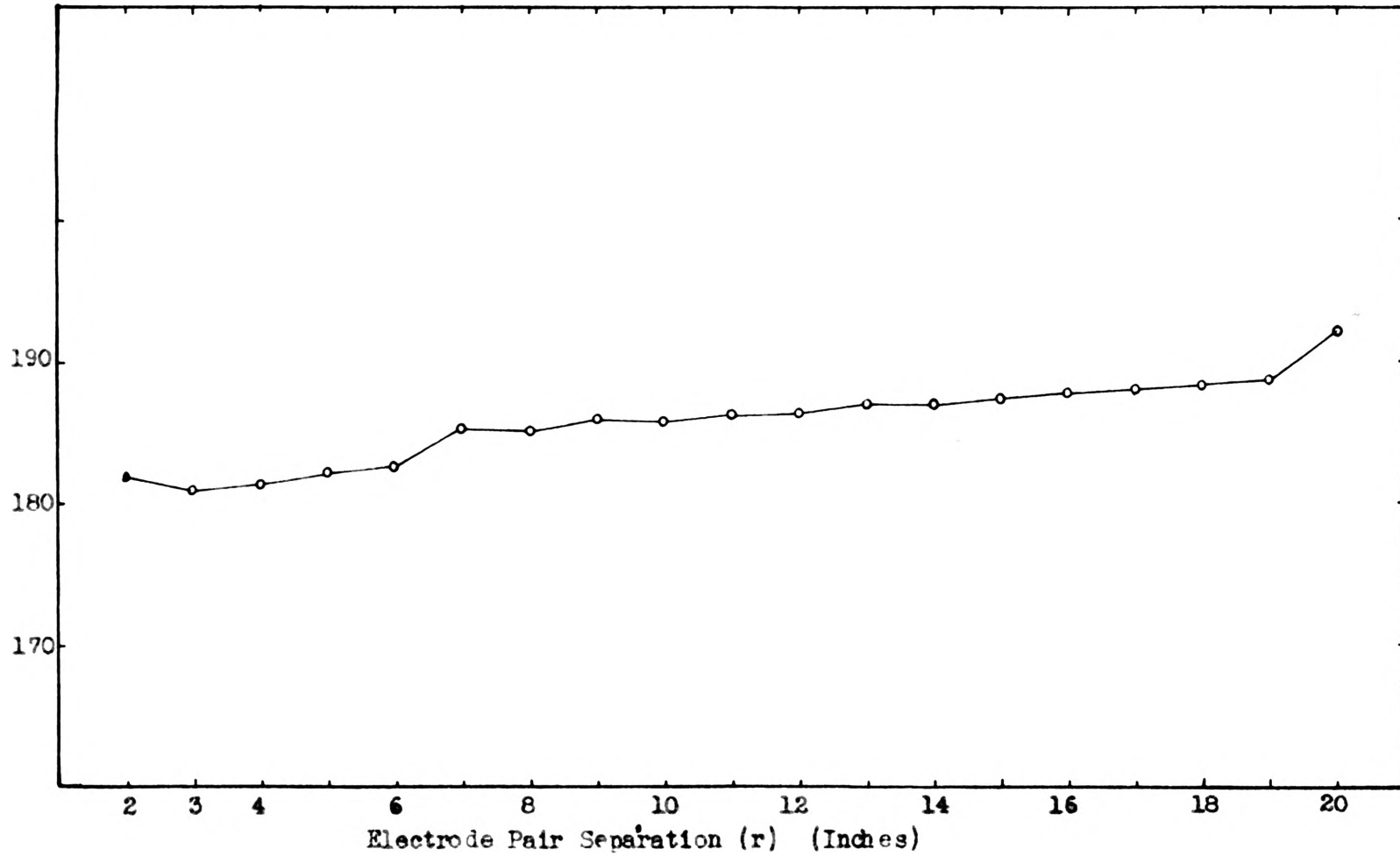Fig. 7-1 A-configuration Depth Probe Over The
Homogeneous Brine Water

Fig. 7-2 B-configuration Depth Probe Over
The Homogeneous Brine Water

to two digits. The third digit was obtained by estimating decimal fractions of a linear scale by eye. Therefore the third digit is inaccurate. This limits the accuracy of obtained resistivity values, especially when the A-configuration is applied with large (r) values. The configuration factor (F) is very large, therefore inaccurate estimation of the third digit will greatly affect the obtained resistivity value.

It was also noticed that a reading error, always negative, was greater when the resistance was small. A resistance of 0.950 ohms indicated on the lowest reading scale, 0-1 ohm, is indicated as only 0.90 ohms when the range selector is switched to a ten times larger scale, 0-10 ohms. This effect appears in the A-configuration measurements where the reading of (R) decreases with the increase of (r). In contrast, the configuration factor (F) for the A-configuration increases when (r) is increased. Therefore small readings of (R) from the Megger Tester for the A-configuration are exaggerated by multiplying (F) and the effect will appear as a downward curve when apparent resistivity values are plotted against the value of (r). Figure 7-1 shows a downward curve where the curve is theoretically a straight line.

When (r) was expanded to 10a, the value of (R) as measured by the Megger Tester was very close to zero. This limits the depth probe method for the A-configuration within the range of r = 10 a. From this example, it is clear that precision meters should be used in measureing current and potential drops if the A-configuration is applied in the field.

When the brine water was measured with the B—configuration having an electrode pair separation (r) less than five inches, (see Fig. 7-2), the resistivity curve approximated a straight line. There is a sudden increase in the curve when (r) is expanded from 6 to 7 inches, and from 19 to 20 inches. This is probably caused from receiving reflected currents from the bottom and walls of the tank. A. H. Kwentus has made a similar investigation of this tank by using the Wenner configuration. He stated that the bottom effect is negligible when electrode spacing (a) is less than six inches. When the electrode spacing is six inches in the Wenner configuration, the current electrodes are 18 inches apart. This is probably equivalent to 17 inches of (r) separation in the B—configuration. Within this range of electrode spacing, the effect of reflected currents can be assumed negligible.

B.   Two Layer Problem.

To simulate a two layer problem for which the lower layer is highly resistive ($\rho_2 \approx \infty$), a piece of masonite, three feet wide and six feet long, was suspended horizontally in the brine water at a depth of six inches. Depth probing methods, using configurations A and B, were thus applied to measure resistivities over the water surface. Results are given in Tables 7-3 and 7-4. The results are also plotted in curves of resistivity ratio (ρ_a/ρ) versus (r/a), where (ρ_a) is the measured resistivity. See Figures 7-3 and 7-4.

Because the Megger Tester readings are inaccurate when (R) is

Table 7-3

A-Configuration Depth Probe Over a Piece of Masonite Suspended 6 Inches Deep in the Brine Water

Electrode Pair Separation (r) Inches	Apparent Resistivity, (ρ_a) (Ohm-cms)	Resistivity of Brine Water (ρ_i) (Ohm-cms)	Resistivity Ratio (ρ_a/ρ_i)
2	176.8	180.04	0.979
3	172.3	183	0.942
4	172.2	177	0.971
5	156.2	166.7	0.936
6	149.4	159	0.939
7	137.7	147.4	0.945
8	120.7	128.4	0.939
9	120.7	109.2	1.104
10	86.9	79.2	1.100

Table 7-4

B-Configuration Depth Probe Over a Piece of Masonite
Suspended 6 Inches Deep in the Brine Water

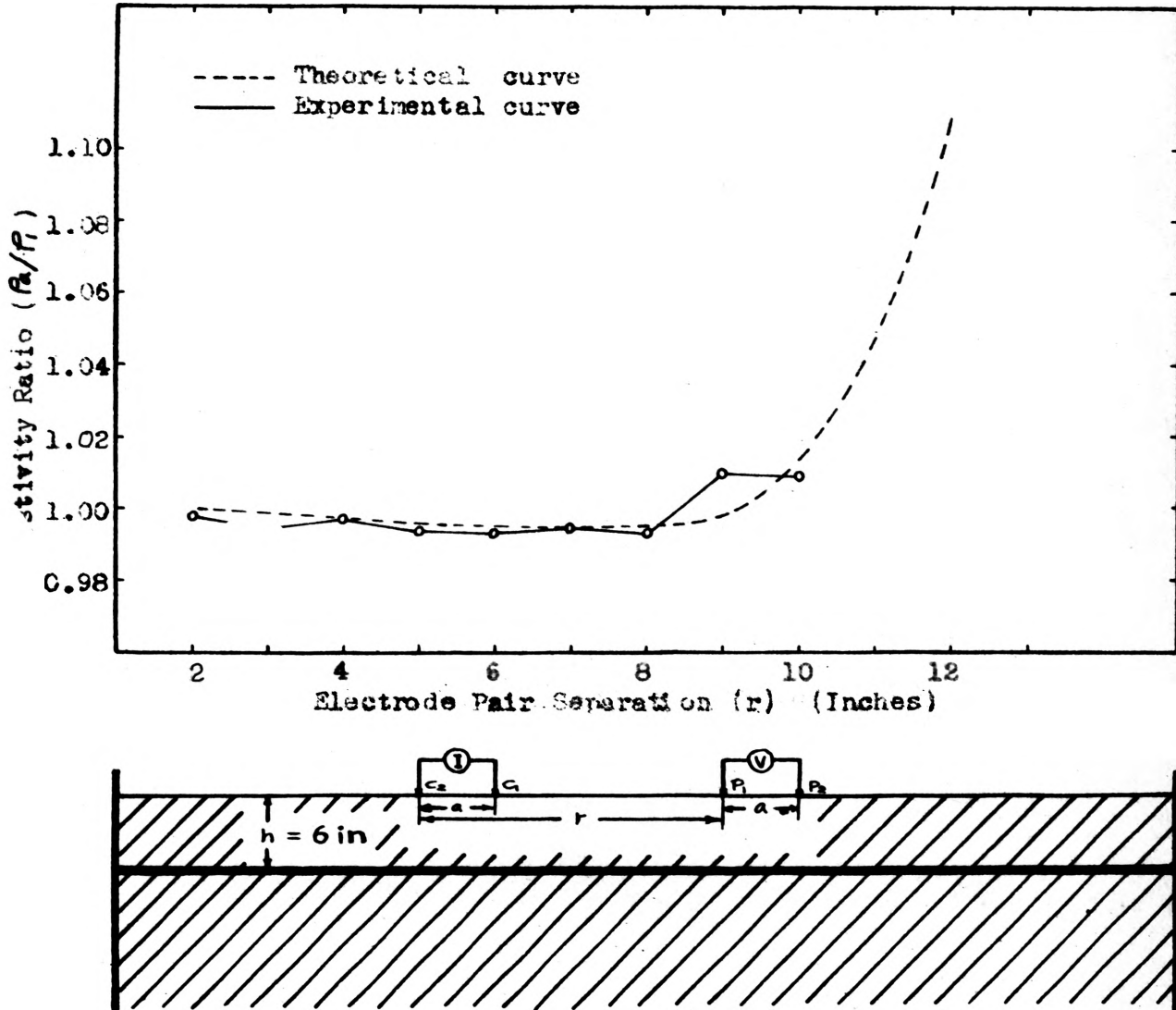| Electrode pair separation (r) Inches	Apparent Resistivity (ρ_a) Ohm-cms	Resistivity of brine water (ρ_i) Ohm-cms	Resistivity ratio (ρ_a / ρ_i)
2	185.3	182	1.020
3	187	181	1.032
4	186.5	181.3	1.028
5	188.4	182.4	1.033
6	190.8	182.8	1.045
7	191	185	1.030
8	192.3	185	1.038
9	192.8	185.6	1.037
10	195.3	185.4	1.052
11	196.9	186	1.057
12	199.5	186.2	1.071
13	200.5	187	1.073
14	202.2	187.3	1.080

Fig. 7-3 A-configuration Depth Probe over the Brine Water
With a Piece of Masonite Horizontally Suspended
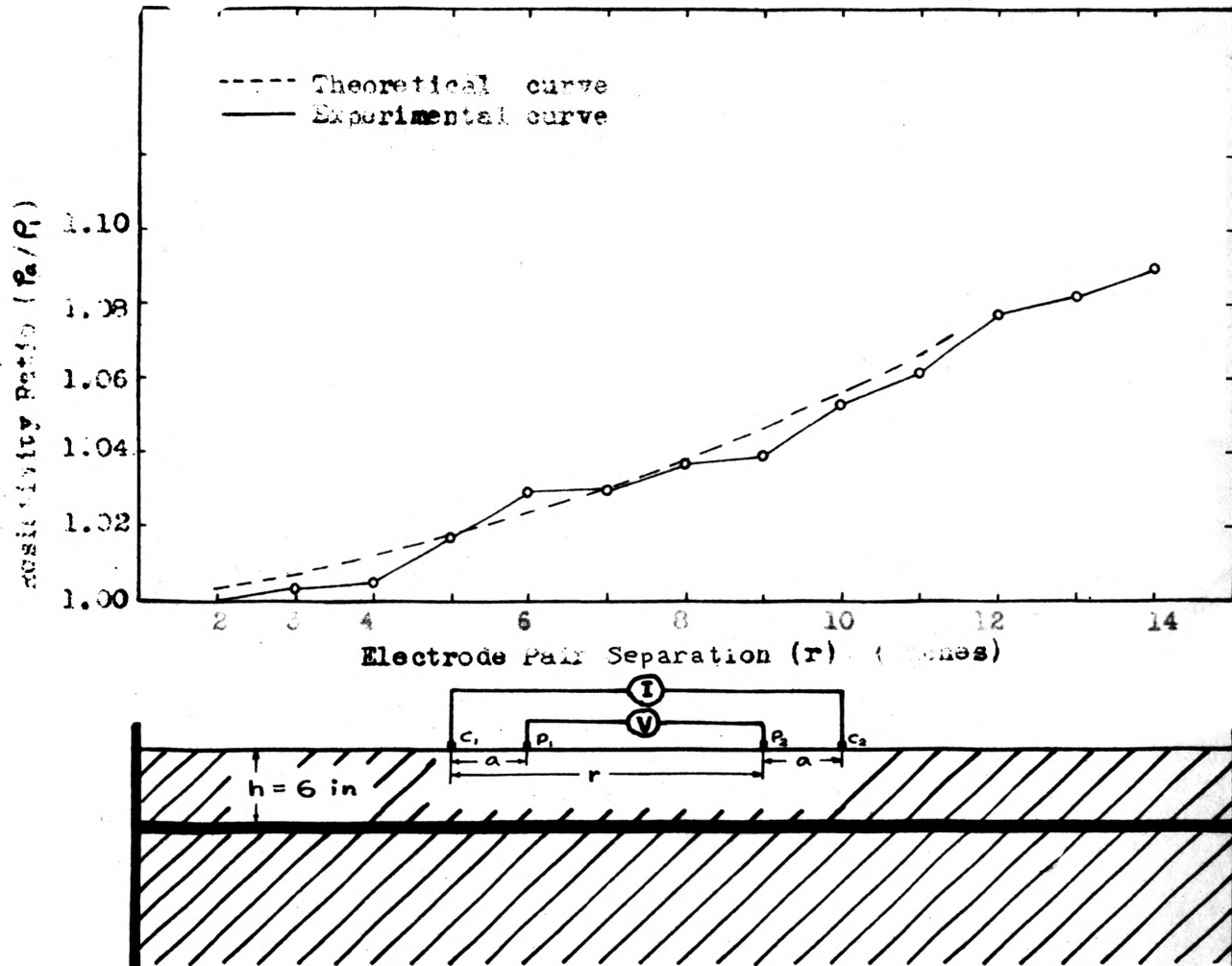at 6 Inch Depth

Fig. 7-4   B-configuration Depth Probe Over the Brine Water
          With a Piece of Masonite Horizontally Suspended at
          6 Inches Depth.

small, it is impossible to obtain an average resistivity ρ_i of the brine water, for use in the ratio (ρ_a/ρ_i). In order to obtain the effect of current reflected from the second layer, the resistivity ratio, ρ_a/ρ_i, was obtained by taking the ratio of two measured resistivity values at the same separation (r). The value (ρ_a) is the resistivity value when masonite is suspended and (ρ_i) is the resistivity value without masonite. Thus the values of (ρ_i) are simply obtained from Table 7-1 and 7-2. Comparing the obtained curves of new configurations, the experimental curves are very close to theoretical curves.

Comparing Figures 7-3 and 7-4, one can see that the A-configuration has better resolution than the B-configuration. The second layer effect appears in the A-configuration curve at r = 9 a and rapidly increases. In other words, the effect appears when h = 1.5 r, (h) being the thickness of the upper layer, and increases when (r) is further increased. Because the effect appears sharply, the A-configuration is useful for two layer problems, but the effect will not become apparent until the value of (r) is expanded larger than 1.5 (h).

C.   Vertical Dyke Problem.

To simulate a vertical dyke of small thickness and high resistivity, a piece of masonite 1/4 inch thick, 3 feet wide, and 18 inches high, was suspended vertically across the center of the tank. Lateral traversing of (a) = 1 inch and (r) = 5 inches was taken using both the A- and B-configuration. The traverses were taken perpendicular to the plane of the masonite. The resistivity values measured at

various distances along the traverses are presented in Tables 7-5 and 7-6. The data of ρ_a/ρ_i are plotted versus the distance from the edge of the dyke in Figures 7-5 and 7-6. Both curves agree closely with their theoretical curve equivalents. The values within (d) = -2 to (d) = + 2 1/4 inch in the B-configuration curve (Fig. 7-6) are rather small where theoretically these values are infinitely large. This results from the current leaking across the dyke by passing around, under and through the masonite board. In the calculation for the theoretical curve the dyke was assumed to be a perfect insulator.

Comparing Figures 7-5 and 7-6, it is noted that the shape of the curve for the A-configuration is reversed from that of the B-configuration. This is due to difference in the electrode arrangement of the two configurations. If the current electrodes are expressed as (C) and the potential electrodes as (P), than the electrode configuration is CCPP in the A-configuration and CPPC in the B-configuration. The theoretical analyses of these electrode arrangements for the Wenner configuration was made by E. W. Carpenter (1955).

D. Conclusion

The theoretical curves obtained from the equations derived in the preceding chapters are well supported by these model experiments of these simplified geologic conditions. For the two layer problem, the theoretical and experimental A-configuration curves show the effect of the second layer more clearly than those for the B-configuration.

Table 7-5

A-Configuration Lateral Traverse Across a Vertical Masonite $\frac{1}{4}$ Inch Thick and Suspended in the Brine Water. $r = 5$ a, The Resistivity of the Brine Water (ρ_1) is 155.4 Ohm-cms

Distance from the left edge of masonite (d) (Inch)	Apparent resistivity (ρ_a) (Ohm-cms)	Resistivity ratio (ρ_a/ρ_1)
-10	168.84	1.06
-9	160.02	1.02
-8	160.02	1.02
-7	157.99	1.002
-6	155.19	1.00
-5	132.84	0.855
-4	123.70	0.796
-3$\frac{3}{4}$	116.84	0.752
-3$\frac{1}{2}$	107.19	0.690
-3$\frac{1}{4}$	95.00	0.611
-3	85.34	0.550
-2$\frac{3}{4}$	734.06	4.722
-2$\frac{1}{2}$	802.64	5.163
-2$\frac{1}{4}$	873.76	5.620
-2	929.64	5.980
-1$\frac{3}{4}$	25.86	0.166
-1$\frac{1}{2}$	8.69	0.056
-1$\frac{1}{4}$	2.87	0.019
-1	.0.96	0.006
-$\frac{1}{2}$	0	0
0	0	0
$\frac{1}{2}$	0	0
1	0	0
1$\frac{1}{4}$	0	0
1$\frac{1}{2}$	2.87	0.019
1$\frac{3}{4}$	6.71	0.043
2	12.42	0.080
2$\frac{1}{4}$	967.74	6.22
2$\frac{1}{2}$	883.92	5.686
2$\frac{3}{4}$	825.50	5.311
3	746.76	4.804
3$\frac{1}{4}$	87.88	0.565
3$\frac{1}{2}$	105.16	0.676
3$\frac{3}{4}$	107.19	0.690
4	177.86	0.760
4$\frac{1}{4}$	123.44	0.794
5	135.89	0.874
5$\frac{1}{4}$	141.73	0.912
6	148.34	0.954
7	148.34	0.954
8	150.37	0.967
9	151.13	0.972

Table 7-6

B-Configuration Lateral Traverse Across a Vertical Masonite $\frac{1}{4}$ Inch Thick and Suspended in the Brine Water. $r = 5$ a, Resistivity of the Brine Water (ρ_i) is 182.4 Ohm-cms

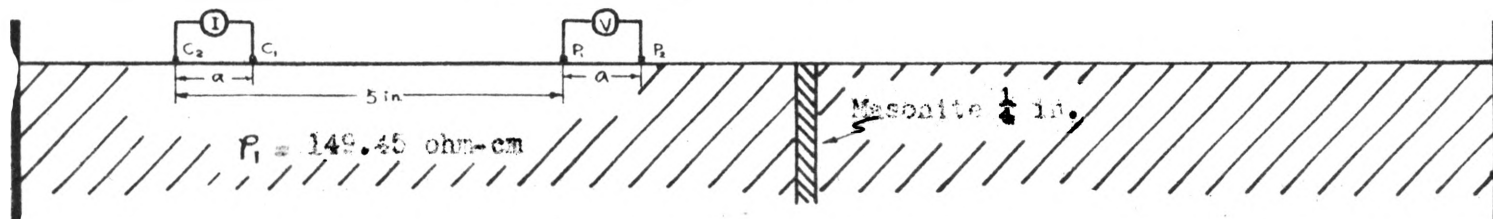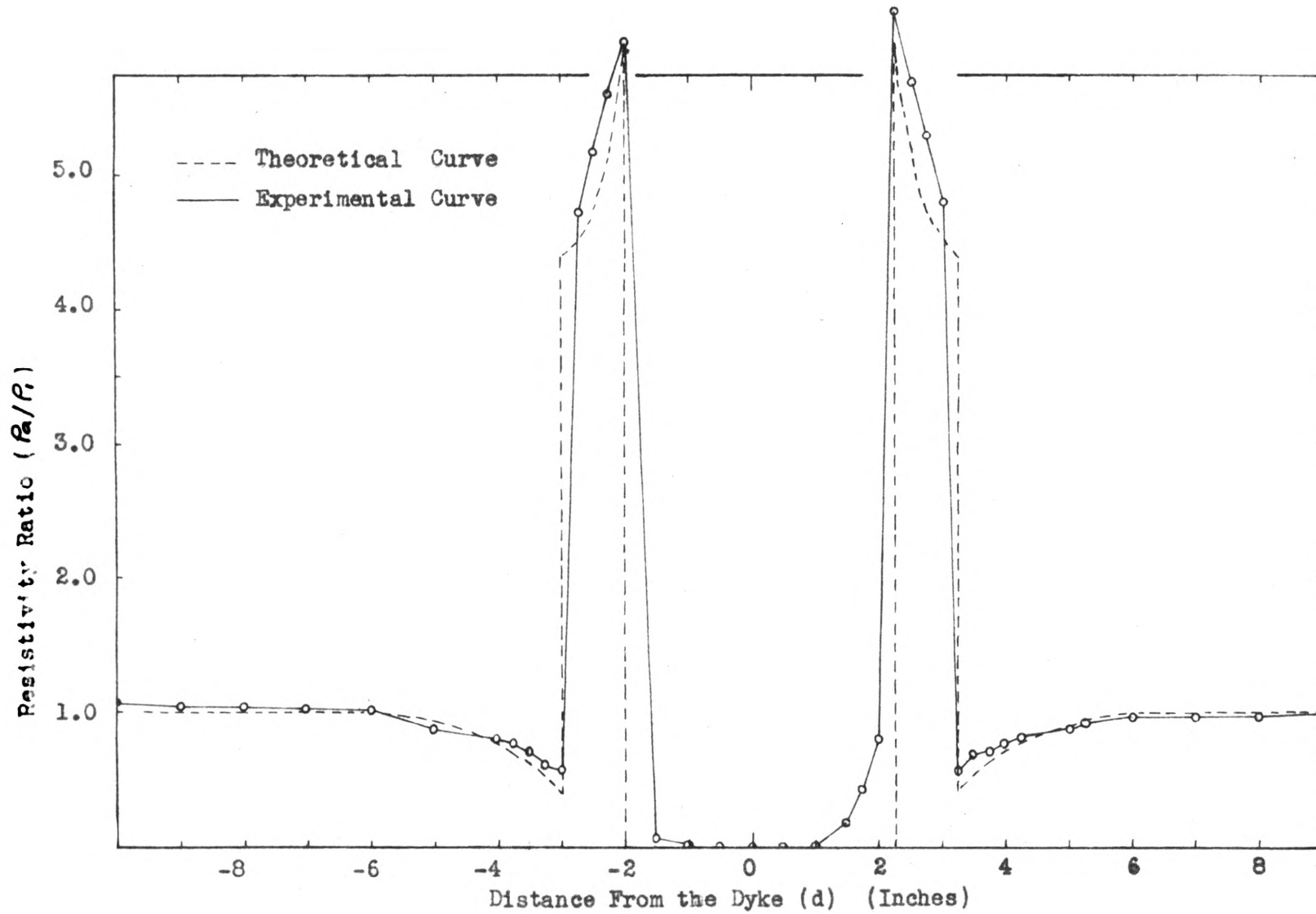| Distance from left edge of the masonite (d) (Inch)	Apparent Resistivity (ρ_a) (Ohm-cms)	Resistivity Ratio (ρ_a/ρ_i)
-15	182.37	1
-13	182.37	1
-12	182.37	1
-11	182.37	1
-9	182.37	1
-7	182.63	1
-6	185.67	1.02
-5	188.72	1.03
-4	196.60	1.08
$-3\frac{3}{4}$	201.68	1.11
$-3\frac{1}{2}$	210.57	1.15
$-3\frac{1}{4}$	213.61	1.17
-3	253.75	1.39
$-2\frac{3}{4}$	96.01	0.526
$-2\frac{1}{2}$	90.68	0.497
$-2\frac{1}{4}$	90.17	0.494
-2	93.73	0.514
$-1\frac{3}{4}$	313.44	1.718
$-1\frac{1}{2}$	319.53	1.752
-1	320.04	1.754
$-\frac{1}{2}$	284.48	1.559
0	284.99	1.549
$\frac{1}{2}$	284.99	1.549
1	291.59	1.599
$1\frac{1}{2}$	307.59	1.687
$1\frac{3}{4}$	324.36	1.779
2	346.46	1.900
$2\frac{1}{4}$	93.98	0.515
$2\frac{1}{2}$	91.95	0.504
$2\frac{3}{4}$	93.47	0.513
3	111.76	0.613
$3\frac{1}{4}$	249.68	1.369
$3\frac{1}{2}$	220.47	1.209
4	203.71	1.117
$4\frac{1}{4}$	199.64	1.095
5	190.25	1.043
6	186.69	1.024
7	182.63	1.001
8	182.63	1.001
9	182.63	1.001

Fig. 7-5 A-configuration Lateral Traverse Across a Piece of Masonite Vertically
uspended In The Brine Water

82

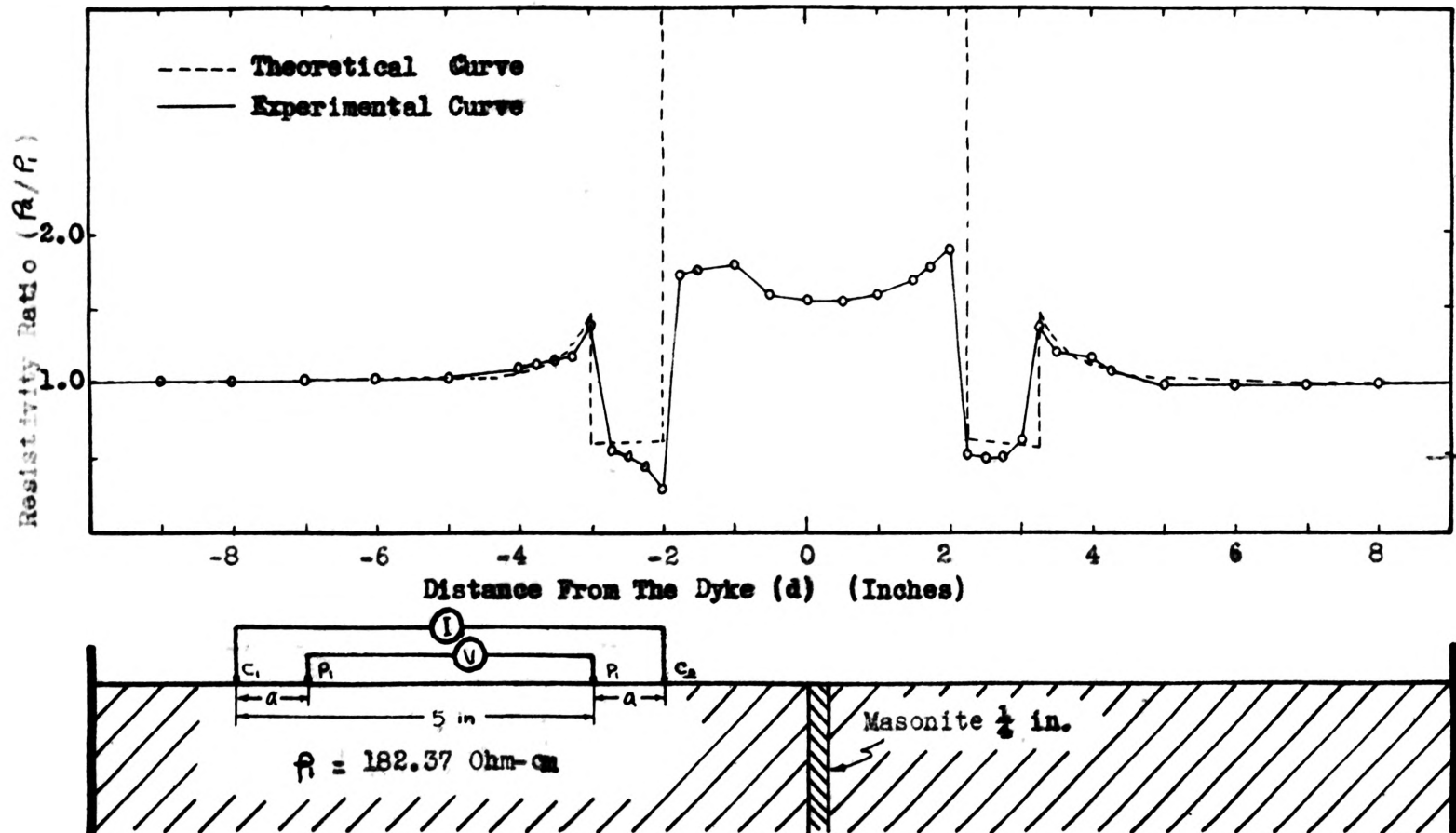Fig. 7-6 B-configuration Lateral Traverse Across a Piece of Masonite
Vertically Suspended In The Brine Water

Because the effect appears sharp in the A-configuration curve, so
the determination of the depth of the second layer by the A-configuration
will be easier than that by the B-configuration.

Theoretical curves for the vertical dyke will match those of
experimental curves for both A- and B-configuration.

VIII. CONCLUSIONS

The results of this investigation show that the application of either the A-configuration or the B-configuration to electrical resistivity work presents no particular difficulty. It was possible to derive equations for resistivity for a homogeneous medium by applying the equations for the potential at a point. For the new configurations the equations found are functions of fixed electrode spacing, (a) and the electrode pair separation, (r):

$$\rho_a = \frac{\Delta V}{I}\, 2\pi \left[\frac{r(r^2-a^2)}{2a^2}\right] \quad \text{for the A-configuration}$$

and

$$\rho_a = \frac{\Delta V}{I}\, 2\pi \left[\frac{ar}{2(r-a)}\right] \quad \text{for the B-configuration}$$

An error in the measurement of (r) has a greater effect on the value of apparent resistivity in the A-configuration than in the B-configuration, because the third power of (r) is used in the apparent resistivity equation for the A-configuration, and the first power of (r) is used in the B-configuration equation. The measured ($\Delta V/I$) is smaller for the A-configuration than for the B-configuration, so more precise instruments are required for the A-configuration. Except for this difficulty in measuring ($\Delta V/I$), there is no particular difficulty in applying these configurations to field operations. Because the distance within an electrode pair remains constant, it may be relatively simple to mount an electrode pair on a mobile vehicle. For the A-configuration, it would not be necessary to connect the vehicle carrying the current electrodes to that carrying

the potential electrodes. However, it would be necessary to provide some means of measuring the vehicle separation. It would appear that the A- and B-configurations can be more easily applied to field operations than the Wenner configuration.

Theoretical apparent resistivity values over two simple hypothetical geologic structures, a two layered earth and a vertical fault plane, were derived by applying Maxwell's theory of images. Solutions were found for both the A- and B-configurations.

For the sturcture of two horizontal layers, a depth probe method of expanding the electrode pair separation was used. The change in apparent resistivity due to the second layer was stronger for the A-configuration than for the B-configuration. The magnitude of the effect for the B-configuration is smaller than that of the Wenner configuration, and approaches 1/2 that of the Wenner configuration when the electrode pair separation is large.

Theoretical solutions for the new configurations were derived for traversing across a vertical fault plane with a fixed electrode separation. Apparent resistivity equations for five different positions of the electrode configuration relative to the fault plane were derived. Graphs of apparent resistivity across the fault plane indicate that both configurations clearly reveal the effect of the discontinuity.

The theoretical apparent resistivity curves were tested by measuring the apparent resistivities of models of the simplified geologic structures. The measured resistivitites agreed very closely with those predicted by the derived equations.

BIBLIOGRAPHY

Aldr dge, R. F. (1937) The Effect of Dipping Strata on Earth-Resistivity Determinations. Colorado School of Mines Quarternary, v.32, p.171-186.

Carpenter, E. W. (1955) Some Notes Concerning Wenner Configuration. Geophysical Prospecting, v.3, p.388-402.

Cook, K. L. and R. Van Nostrand (1954) Interpretation of Resistivity Data over Field Sinks. Geophysics, v.19, p.761-790.

Eve, A. S., D. A. Keys and E. W. Lee (1929) Depth Attainable by Electrical Methods in Applied Geophysics. U. S. Bureau of Mines, Technical Papers No.463, p.1929.

Evjan, H. M. (1938) Depth Factors and Resolving Power of Electrical Measurements. Geophysics, v.3, p.38.

Harnwell, G. P. Principles of Electicity and Electromagnetism. McGraw Hill, p.58.

Hedstrom, H. (1932) Electrical Prospecting for Auriferous Quartz Veins and Reefs. Mining Magazine, v.46, p.201.

Heiland, C. A. (1940) Geophysical Exploration. Prentice Hall, New York, p.707-744.

Hubbert, K. M. (1934) Earth-Resistivity Surveying in Illinois. A.I.M.E. Transactions, v.110, p.1-39.

_____ (1934) Location of Faults in Hardin County Illinois, by the Earth Resistivity Method. A.I.M.E. Transactions, v.110, p.40-48.

Hummel, J. N. (1932) A Theoretical Study of Apparent Resistivity in Surface Potential Methods. A.I.M.E. Transactions, 1932, p.392-422.

Jakosky, J. J. (1938) Method and Apparatus for Electrical Exploration of the Subsurface. U. S. Patent No. 2,105,247.

_____ (1957) Exploration Geophysics. Trija Publishing Co., California, p.471-529.

Jameson, M. H. (1945) Effect of Dipping Strata on Determination of Potential-Drop-Ratio Method. A.I.M.E. Transactions, v.164, p.164-169.

Jeans, J. H. (1925) Electricity and Magnetism. University Press, Cambridge, England, 5th edition.

Kwentus, A. H. (1960) Electrical Model Investigations Using the Horizontal Profiling Technique. Master s Thesis, Missouri School of Mines.

Lancaster-Jones, E. (1930) The Earth Resistivity Method of Electrical Prospecting. Mining Magazine, v.43, p.19-23.

Lee, F. W. (1928) Measuring the Variation of Ground Pesistivity with a Megger. U. S. Bureau of Mines Technical Paper, No.440.

Logn, O. (1954) Mapping nearly Vertical Discontinuities by Earth Resistivities. Geophysics, v.19, p.739-760

Low, B., S. F. Kelly and W. B. Creagmile (1932) Applying the Megger Ground Tester in Electrical Exploration. A.I.M.E. Transactions, 1932, p.114-125.

Maeda, K. (1955) Apparent Resistivity for Dipping Beds. Geophysics, v.20, p.123-147.

Maxwell, J. M. (1891) A Treatise on Electricity and Magnetism. v.1, New York, 4th edition, Art 161 and p.315-318.

Peters, L. J. (1930) The Solution of Some Theoretical Problems which Arise in Electrical Methods of Geophysical Exploration. Bulletin, University of Wisconsin, Engineering Experiment Station Series, No.71.

Roman, I. (1931) How to Compute Tables for Determining Electrical Resistivity of Underlying Beds and their Application to Geophysical Problems. U. S. Bureau of Mines, Technical Paper No. 502.

_____ (1933) The Calculation of Electrical Resistivity for a Region Underlying two Uniform Layers. Terrestrial Magnetism and Electricity, v.38, no.2, p.118 and no.3, p.185.

_____ (1941) Superposition in the Interpretation of Two-Layer Earth-Resistivity Cruves. U. S. Geological Survey, Bulletin 927A.

_____ (1953) Resistivity Reconnaissance. American Society of Testing Materials, Special Technical Publication No.122, Symposium of Surface and Subsurface Reconnaissance, p.171-220.

_____ (1959) An Image Analysis of Multiple Layer Resistivity Problems. Geophysics, v.24, p.485-509.

_____ (1960) Apparent Resistivity of a Single Uniform Overburden. U. S. Geological Survey, Professional Papers, 365.

Sanjeevareddi, B. S. (1936) A Theoretical and Experimental Investigation of the Earth-Resistivity Method as Applied to Dipping Strata. Master s Thesis, Colorado School of Mines.

Schlumberger, C. M. (1929) Depth of Investigation by Potential Methods of Electrical Exploration. A.I.M.E. Transactions, 1932, p.127.

Skalaskaya, I. P. (1948) The Field of a Point Source of Current Situated on the Earth s Surface above an Inclined Plane. Journal of Technical Physics, U.S.S.R., v.18, p.1242-1254.

Smythe, W. R. (1950) Static and Dynamic Electricity. 2nd edition, McGraw Hill.

Tagg, G. F. (1930) The Earth Resistivity Method of Geophysical Prospecting, Some Theoretical Considerations. Mining Magazine, v.43, p.150-158.

_____ (1934) Interpretation of Resistivity Measurements. A.I.M.E. Transactions, v.110.

Unz, M. (1953) Apparent Resistivity Curves for Dipping Beds. Geophysics, v.18, p.116-137.

Watson, R. J. (1934) A Contribution to the Interpretation of Resistivity Measurement Obtained from Surface Potential Observations. A.I.M.E. Transactions, Geophysical Prospecting, Technical Publication No. 518, p.201.

_____ (1932) Mathematical Theory of Electrical Flow in Stratified Media with Horizontal Homogeneous and Isotropic Layers. A.I.M.E. Transactions, 1932, p.423.

Wenner, F. (1915) A Method of Measuring Earth Resistivity. Bulletin, Bureau of Standards, v.12, p.469-478.

VITA

The author was born in Chia-Yi, Taiwan, on June 14, 1934. After attending elementary school in Chia-Yi, he entered the Taiwan Provincial Chia-Yi High School. In September 1953, he was admitted to the Taiwan Provincial Cheng Kung University. In July, 1957, he received a Bachelor of Science Degree in Mining Engineering from the same University. After graduation he received the R. O. T. C. training at the Fung-Shan Military School and then served in the Chinese Army; he was honorably discharged in March, 1959.

In September, 1959, the author came to the United States to enter the Missouri School of Mines and Metallurgy. He is pursuing graduate study leading to a degree of Master of Science in Mining Engineering. He is an associate member of Sigma Xi, a member of Sigma Gamma Epsilon, and has student membership in the Society of Exploration Geophysicits and the American Geophysical Union.